Astron. Astrophys. 300, 237-258 (1995)

ASTRONOMY
AND
ASTROPHYSICS

Chemical composition of Wolf–Rayet stars

II. Hydrogen-to-helium ratio

T. Nugis[1,2] **and A. Niedzielski**[2]

[1] Tartu Astrophysical Observatory, EE2444 Tõravere, Estonia
(e-mail address: nugis@jupiter.aai.ee)
[2] Institute of Astronomy N. Copernicus University, ul. Chopina 12/18, PL-87-100 Toruń, Poland
(e-mail address: aniedzi@astri.uni.torun.pl)

Received 13 May 1994 / Accepted 26 January 1995

Abstract. The formation of He II, He I and H I lines in the winds of some representative WN stars of different spectral subtypes has been modeled. Two different types of models were studied: the clumped winds and smooth winds for both of which the standard velocity law $v = v_0 + (v_\infty - v_0)\left(1 - R_*/r\right)^\beta$ with $\beta = 1$ was assumed. The smooth winds model predicts about two times lower IR fluxes than observed if one determines the matter density in the winds through the observed values of radio fluxes. The increased density smooth wind models with 1.5 times higher density as compared to the radio-flux scaling are in reasonable agreement with IR fluxes and He II and He I line fluxes in the case of WN 5, WN 6 and WN 8 stars but for other subtypes these models predict discrepant line fluxes. The clumped wind models agree quite well with the most important observational data whereas somewhat lower mass loss rates are now derived as compared to the smooth wind models. Theoretical line fluxes were found by summing of the contributions from different layers of the wind. The statistical equilibria equations for level populations were solved in the Sobolev approximation by taking into account the overlap of He II and H I lines in the expanding medium. We used 40, 20 and 52 level atomic models for He II, H I and He I respectively, whereas the influence of higher levels was taken into account through the correction terms. On the basis of our modelling study we derived a simple formula for the determination of hydrogen-to-helium ratios for WN stars which was used for concrete estimates for 28 stars. In all cases the hydrogen-to-helium ratios are lower than the mean cosmic value. By inspection of the line fluxes of the neighboring He II lines of $(n-4)$, $(n-6)$ and $(n-8)$ series in the spectra of two WC stars we concluded that no hydrogen seems to be present in their winds. The hydrogen-to-helium ratio is decreasing when going from late to early WN subtypes with strong scatter existing among the stars of WN 6 and later subtypes.

Send offprint requests to: T. Nugis

Key words: stars: abundances – stars: mass-loss – stars: Wolf-Rayet

1. Introduction

The Wolf-Rayet (WR) stars are believed to be the end points of the evolution of the most massive stars (van der Hucht 1992), but their temperatures and luminosities are not precisely known. Therefore, they are sometimes regarded even as pre-main sequence objects (Underhill 1991). The reason for such discrepancies is that in the optical wavelength range we observe not a star itself, but a sum of the stellar radiation and that of the dense and extremely fast expanding envelope, where a variety of physical processes is displayed. Optical spectra of WR stars are therefore weakly coupled to the basic stellar parameters of mass and luminosity.

The classification of WR stars is based upon the appearance of optical emission lines of different ions of helium, carbon, nitrogen and oxygen. Beals & Plaskett (1935) and later on Smith (1968a), arranged these stars into two sequences - the one in which the helium and nitrogen lines dominate (the WN class) and the other one in which the helium, carbon and oxygen lines dominate (the WC class). Barlow & Hummer (1982) identified a new subtype related to the WC class, with extremely strong oxygen lines - WO stars. Within these three sequences WR stars can be further subdivided into higher and lower excitation subtypes, depending on the strengths of lines of the various ions of helium, nitrogen, carbon and oxygen. These range from WN 2 to WN 9, from WC 4 to WC 9, and from WO 1 to WO 4. Ionization state in the winds of WR is mainly determined by stellar effective temperature and wind density, but coronal heating may also play an important role.

The WN and WC sequences depict as usually concluded different elemental abundances, the former displaying the properties of core hydrogen burning "equilibrium" values, and the latter that of the even more evolved helium burning material (Smith & Hummer 1988; Nugis 1988). Nevertheless, up to the recent times some attempts have been made to prove that WR stars have a normal chemical composition, and that the differences of WN and WC spectra are due to the different excitation conditions in the outer layers of these stars (Bhatia & Underhill 1988).

Emission lines and violet-shifted P Cygni absorptions observed in the spectra of WR stars originate in the envelope. An envelope is defined as an expanding and continuously renewing outer region of the star which is formed by the more or less constantly blowing stellar wind. The inner limit of the envelope coincides with the radius of the stellar core which is defined as a region of formation of a stellar continuous spectrum and a photospheric absorption spectrum (unshifted absorption lines). In the spectra of WR stars no photospheric lines have definitely been observed. These stars are losing matter very intensively ($\dot{M} \sim 10^{-5} \div 10^{-4} M_{\odot}\mathrm{yr}^{-1}$) and the inner regions of winds with low expansion velocities (v being close to the sound velocity) are in most cases not seen at all because the optical depth of the above-lying layers is (much) higher than unity for absorption in the continuum. The continuous spectrum of WR stars is due to stellar and envelope contributions. At long wavelengths, due to the rapid increase of the absorption coefficient with wavelength ($\kappa \propto \lambda^2$), more and more distant regions of the envelope become optically thick in the continuum. This circumstance must be taken into account when carrying out a modelling study of WR stars. In the observable spectral range the optical depth of the envelope due to true absorption in the continuum (caused by bound-free and free-free transitions in the ionized plasma) is the smallest in the short-wavelength range of the observable UV spectral region ($\lambda\lambda$ 1000 $\sim$ 2000 Å).

It is known that the UV continua of WR stars are seriously blended by the lines of iron ions. We have studied this problem carefully. Fortunately, there exist some intervals in that spectral region which are free of lines. These intervals were selected and published in the paper of Nugis (1990b) and they are used for the estimates of T_c(UV).

From the UV continua we can get information mainly about the star itself and from emission-line spectra, far-IR and radio continua we can get information mainly about the wind (envelope) influenced by the radiation field of the star.

Reliable estimates of the hydrogen-to-helium ratio in the outer layers (winds) of WR stars are very important for clarifying the evolutionary status of these stars. A historical overview is given in Nugis (1991). Although it is more or less commonly accepted that WR stars are chemically far evolved stars, in different studies of the line spectra strongly different results have sometimes been obtained. Some authors have even estimated that the hydrogen-to-helium ratio in the winds of WR stars is more or less normal (Bhatia & Underhill 1986) or at least that this may be so in late type WN stars (Vreux et al. 1989, 1990). For WN 8 star HD 96548 Vreux et al. (1989) estimated that the $N(\mathrm{H}^+)/N(\mathrm{He}^{++}) \sim 10$ (by number) from the study of near IR lines of the higher members of the He II (k – 6) series by assuming that the wind is optically thin for radiation in these transitions. Hamann et al. (1991) and Crowther (1993) found for the same star by a wind modelling study that $N(\mathrm{H})/N(\mathrm{He}) \sim 0.7$, and Nugis (1988, 1991) estimated for two WN 8 stars by limit-decrement method applied to the Pickering series that $N(\mathrm{H})/N(\mathrm{He}) \sim 0.7 \div 1.5$.

Qualitative evaluation of the previous estimates of H/He ratios obtained by simple methods is presented in Sect. 2. The empirical wind modelling scheme and scaling rules are described in Sect. 3. The formulae which are needed for taking into account the clumped nature of the winds are presented in Sect. 4. The observational data used by us are described in Sect. 5. The results of our empirical modelling study of the representative stars of different WN subtypes are analyzed in Sect. 6 and the method and results of the H/He ratio estimates for 28 WN stars are presented in Sect. 7. The general discussion is presented in Sect. 8 and the atomic data used by us are described in the Appendix.

2. Qualitative considerations

The energy emitted in some unblended He II line by the envelope with the volume V can be expressed in the form:

$$E_{ki} = \int_V f_c(1-W)N_k A_{ki}\beta_{ik}h\nu_{ik}dV \quad , \tag{1}$$

where the term $(1-W)$ accounts for the screening by the star of the part of the envelope lying behind the star (W is the geometrical dilution coefficient), β_{ik} is the line escape probability coefficient, N_k is the level population number density, ν_{ik} is the line frequency and A_{ki} is the Einstein coefficient for spontaneous emission. The factor f_c accounts for the dilution of the line emission due to electron scattering and continuum absorption by the above-lying layers in the envelope.
The line intensity I_{ki} is defined as the amount of the energy emitted in the line by unit volume at the distance r:

$$I_{ki} = N_k A_{ki} h\nu_{ik}\beta_{ik} \quad , \tag{2}$$

therefore

$$E_{ki} = \int_V f_c(1-W)I_{ki}dV \quad . \tag{3}$$

Let us introduce the term:

$$I'_{ki} = \frac{I_{ki}}{N_e N^+} = z_k A_{ki} h\nu_{ik}\beta_{ik} \quad , \tag{4}$$

$$z_k = \frac{b_k g_k h^3 e^{\frac{I_k}{kT_e}}}{2(2\pi m_e k T_e)^{3/2}} \quad , \tag{5}$$

where b_k is the Menzel departure coefficient, g_k is the statistical weight, T_e is the electron temperature, N_e is the number density of free electrons, N^+ is the number density of ions (He^{++} in the present case) and I_k is the ionization energy of the level k. Let us further introduce the term:

$$I^\circ_{ik} = z^\circ_k A_{ki} h\nu_{ik} \quad , \tag{6}$$

where

$$z_k^{\circ} = \frac{g_k h^3 e^{\frac{I_k}{kT_e}}}{2(2\pi m_e kT_e)^{3/2}} \quad . \tag{7}$$

We have that:

$$I_{ki} = I'_{ki} N_e N^+ = I^{\circ}_{ki} N_e N^+ b_k \beta_{ik} \quad . \tag{8}$$

The energy emitted in the line and the line flux F_{ki} are related through the relationship:

$$F_{ki} = \frac{E_{ki}}{4\pi d^2} \quad , \tag{9}$$

where d is the distance to the star.

From observations we can determine the line flux as:

$$F_{ki} = W_\lambda f_\lambda 10^{0.4A_\lambda} \quad , \tag{10}$$

where f_λ is the observed continuum flux, the term $10^{0.4A_\lambda}$ removes the interstellar extinction and W_λ is the equivalent width of the emission line. The equivalent widths must be corrected for the blue-shifted P Cygni absorption, if present. The full energy emitted by the He II line blended with the H I line (even-even transitions of He II) can be written in the form (the contribution of the lines of other elements must be removed if necessary):

$$E_{ki}^{\mathrm{HeII+HI}} = E_{ki}^{\mathrm{HeII}} + E_{mn}^{\mathrm{HI}} \qquad (m = k/2\ , n = i/2) \quad , \tag{11}$$

where

$$E_{ki}^{\mathrm{HeII}} = \int_V f_c(1-W) I_{ki} e^{-\overline{\tau}_{nm}^{\mathrm{HI}}} dV \quad ,$$

$$E_{mn}^{\mathrm{HI}} = \int_V f_c(1-W) I_{mn} dV \quad .$$

We are dealing throughout this paper with normal winds, where the velocity of the matter flow increases with the radial distance reaching the asymptotic constant value v_∞ far from the stellar surface. Therefore as $\lambda_{ik} < \lambda_{nm}$, we have that due to envelope expansion at every line of sight for a distant observer $\lambda_{ik}(s) = \lambda_{nm}(s')$ where $s' > s$ (the point s' is situated closer to the observer), i.e. the even-even line radiation of He II is suppressed due to absorption by H I atoms. The population number densities of He II are practically unchanged due to the presence of hydrogen but H I population number densities are influenced by He II and this must be taken into account in solving statistical equilibrium equations for finding level population number densities of H I. At an optically thin limit we have that for odd-odd and odd-even (even-odd) lines of He II :

$$E_{ki}^{\mathrm{HeII}} = \int_V (1-W) I_{ki} dV, \quad (\beta_{ik} = 1, f_c = 1), \tag{12}$$

and for even-even lines:

$$E_{ki}^{\mathrm{HeII+HI}} = \int_V (1-W) I_{ki}^{\mathrm{HeII}} dV + \int_V (1-W) I_{mn}^{\mathrm{HI}} dV \tag{13}$$

$$(\beta_{ik} = 1, \beta_{nm} = 1, e^{-\tau_{nm}} = 1, f_c = 1) \quad .$$

Using Eqs. (12 - 13) we will obtain:

$$\frac{E_{ki}^{\mathrm{HeII+HI}}}{E_{ki}^{\mathrm{HeII}}} \approx 1 + \frac{\overline{b}_m}{x\overline{b}_k} \frac{N(\mathrm{H})}{N(\mathrm{He})} \quad , \qquad x = \frac{N^+}{N_{\mathrm{tot}}(He)} \quad . \tag{14}$$

For all WR stars N_{tot} (H) $\approx N^+$ (H I). In the case of early-type WR stars N_{tot}(He) $\approx N$(HeIII) and $\overline{b_m/xb_k} \approx 1$ at high enough values of k. Therefore, we can estimate the N(H)/N(He) ratio directly from the observed fluxes of neighboring He II + H I and He II lines. In the case of late type WR stars helium is predominantly singly ionized in the envelope and only the part of the envelope lying close to the stellar surface is contributing to the He II line emission and even in these layers helium may not be fully doubly ionized. Therefore, for these stars $\overline{b_m/xb_k} > 1$ and from Eq. (14) only the upper limit for the N(H)/N(He) ratio can be obtained when assuming $\overline{b_m/xb_k} \approx 1$. In the case of late type WR stars we must use the He I lines for the determination of the state of ionization of helium and for finding the effective emitting volumes for the He II lines.

Vreux et al. (1989, 1990) assumed that the envelopes of WN stars (including the stars WN 7 - 9) are optically thin for line radiation in the higher members of the series $(k-6)$ (He II) and $(m-3)$ (H I) and they found that for some late type WN stars the $N(\mathrm{H}^+)/N(\mathrm{He}^{++})$ ratios are close to 10. According to the above given considerations, we must regard these estimates as upper limits for the N(H)/N(He) ratios. High members of the Pickering series lines of some late type WN stars have violet-shifted absorption components and therefore they are not optically thin. Optical depth in a line can be expressed according to Castor (1970) by the formula:

$$\tau_{ik} \propto g_i f_{ik} \lambda_{ik} \left(\frac{N_i}{g_i} - \frac{N_k}{g_k} \right) \quad . \tag{15}$$

For higher members of the He II $(k-4)$ and $(k-6)$ series we have that $\tau_{6k}/\tau_{4k} \approx f_{6k}\lambda_{6k}N_6/N_4 f_{4k}\lambda_{4k}$ and at $k = 15$ this gives $\tau_{6,15}/\tau_{4,15} \approx 5.1 N_6/N_4$ and at $k = 25 - \approx 3.9 N_6/N_4$. In all reasonable models for the envelopes of WR stars the ratios N_6/N_4 are higher or close to unity and therefore higher members of the He II $(k-6)$ series are in every case optically thicker than the Pickering series lines (of the same k) and this means that the lines of the He II $(k-6)$ series are not optically thin in the case of late type WN stars.

Bhatia & Underhill (1986) found by their models that N(H)/N(He) ratios of all types of WR stars are nearly normal ($\approx 5 \div 10$). Their conclusions are based on the comparison of the line fluxes of H_β with the fluxes of neighboring He II lines. This result must be interpreted as an indication of the strong model dependence of theoretical line fluxes of lower members of the Pickering and Balmer line series (compare the results of Hamann et al. 1991 and Bhatia & Underhill 1986). In Fig. 1 the ratios $F_{ki}^{\mathrm{obs}}/I_{ki}^{\circ}$ of the He II lines are compared with the prediction of the decrement run of the Bhatia & Underhill (1986) model. The results for their model are obtained from our computations made with the same one-point Sobolev approximation whereas we took into account a greater number of levels

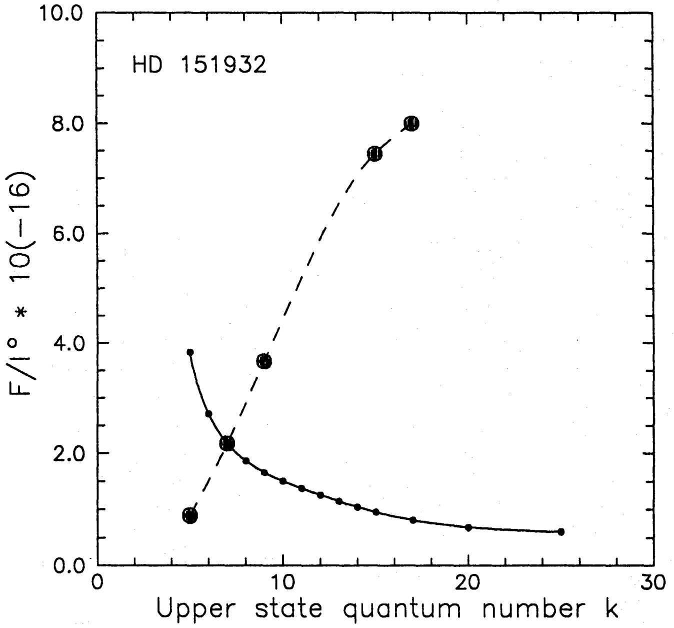

Fig. 1. A comparison of the observed fluxes of the unblended He II Pickering series lines (big dots) with the prediction of the Bhatia & Underhill (1986) model ($T_* = 25\,000$ K, $T_e = 100\,000$ K, $N_e = 10^{10} cm^{-3}$, $dv/dr = 10^{-5} s^{-1}$, normal chemical composition) (small dots) for HD 151932 (WR 153). Given are the fluxes divided by the line intensity $I^{\circ}_{ki} = z^{\circ}_k h\nu_{ik} A_{ki}$ (the observed and model predicted fluxes are adopted to be equal for the line λ5411(7-4)). The Bhatia & Underhill (1986) model predicts an opposite decrement run as compared to the observed one

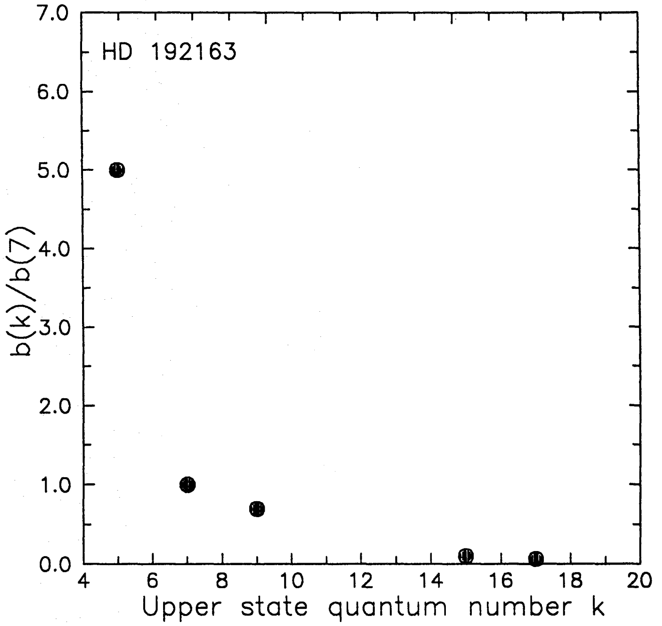

Fig. 2. The optically thick model predicted run of b_k/b_7 for the unblended or weakly blended He II Pickering series lines of the star HD 192163 (WR 136). This run is obtained from Eq. (17) by assuming that the observed and model predicted fluxes are equal for the line λ5411 (7 - 4). The electron temperature is taken to be 22 500 K. The derived run of b_k is not in accord with the shape of line profiles (see the text for details)

in statistical equilibrium equations which enabled us to get information about the line fluxes of higher members of different He II series.

From Fig. 1 it follows that the model of Bhatia & Underhill (1986) predicts the decrement run which is in serious conflict with the observed data. Here it is important to stress that even if we use wrong models we will get in the series limits the same results as in the case of more adequate models. Some problems arise only in the case of late type WR stars for which the asymptotic regime ($\beta_{ik} \to 1$) is not achieved for the highest observable lines of different series.

Most of the strongest He II lines observed in the spectra of WR stars are optically thick. Some simple schemes have been proposed to estimate $N(\mathrm{H})/N(\mathrm{He})$ ratios for the optically thick case. Massey (1980) and Conti et al. (1983) used a simple technique for getting $N(\mathrm{H})/N(\mathrm{He})$ ratios by comparing the observed line fluxes of the even and odd lines of the Pickering series with the theoretical prediction that the line flux is proportional to the effective emitting area with the radius corresponding to the level where the optical depth is unity $\tau_{ik}(\mathrm{HeII}) \simeq 1$ and $\tau_{ik}(\mathrm{HeII + HI}) \simeq \tau_{ik}(\mathrm{HeII}) + \tau_{\mathrm{nm}}(\mathrm{HI}) \approx 1$). Assuming that helium is predominantly doubly ionized in the envelope, we can obtain, following the approach of Massey (1980) and Conti et al. (1983), that:

$$\frac{E^{\mathrm{HeII}}_{ki} + E^{\mathrm{HI}}_{mn}}{E^{\mathrm{HeII}}_{ki}} \approx \left(1 + \frac{N(\mathrm{H})}{N(\mathrm{He})}\frac{b_n}{b_i}\right)^{2/3} . \tag{16}$$

The estimates made by assuming that $b_n/b_i \approx 1$ (as in the above cited papers) cannot be regarded reliable, because the b_i coefficients of the lines of the Balmer and Pickering series (b_2 and b_4) are not equal as a rule. Secondly, in the optically thick limit He II contribution to He II + H I blends ought to be strongly suppressed due to the absorption of the He II line radiation by blending H I atoms (Eq. 11) and this must be taken into consideration when making estimates of $N(\mathrm{H})/N(\mathrm{He})$ ratios by this model.

Instead of the case treated by Massey (1980) and Conti et al. (1983), we may assume that the whole envelope is optically thick for line radiation. In such a case we have that in the blends of He II + H I only H I is present because the line radiation of He II is fully absorbed by H I and the fluxes of He II odd-even lines of some series must approximately follow the relationship (all the lines are assumed to arise at the same effective distance from the stellar surface):

$$\frac{F_{ki}}{F_{ji}} = \frac{b_k}{b_j}\frac{e^{I_k/kT_e}}{e^{I_j/kT_e}}\frac{\lambda^4_{ij}}{\lambda^4_{ik}} . \tag{17}$$

Figure 2 presents the run of b_k/b_7 for the fully optically thick envelope model obtained by assuming that the model predicted flux at λ5411 is equal to the observed value.

From Fig. 2 we can conclude that in the case of a fully optically thick model, the coefficients b_k must strongly decrease with the increase of k for the Pickering series. The same situation appears also in the case of other WN stars. For a very steep decrease of b_k with k, we have that the line source function ($S_{ki} = N_{\rm k}A_{ki}/(N_iB_{ik} - N_{\rm k}B_{ki})$) is very small (even at $T_{\rm e} \rightarrow \infty$) as compared to the stellar radiation power in the continuum and therefore strong absorption components must be observed, especially in the case of weak lines (higher members of some series of lines). But this is not the case and therefore a fully optically thick envelope model cannot be accepted.

We can conclude that the envelopes of WR stars are not fully optically thick and therefore the higher members of at least some line series of He II and H I ought to be more or less optically thin ($\tau_{ik} \rightarrow 0$ if k is high enough). The intensity ratios of more or less optically thin lines are not sensitive to the details of concrete models and therefore these lines are most suitable for a chemical composition study.

3. Modelling scheme

The variability indicative of blob ejection in the winds of WR stars was suggested from the photometry by van Genderen et al. (1987) and was more evidently deduced by spectroscopic observations of systematically varying features superimposed on the broad emission lines (Moffat et al. 1988; Robert & Moffat 1990; Moffat & Robert 1991). Cherepashchuk et al. (1984) (see also Cherepashchuk 1990) found evidence of the presence of a great number of relatively small blobs in interpreting the IR eclipse curve of a WR binary HD 193576 (WN 5 + O 6). IR and radio flux ratios observed in WR stars are in conflict with smooth wind prediction (Nugis 1990a) and they are indicative of a non-standard velocity law or the presence of blobs. The presence of density inhomogeneities is concluded by Hillier (1991) from the weakness of electron scattering wings in strong emission lines.

Antokhin et al. (1992) studied the emission line formation in the clumped wind and concluded that the presence of blobs may seriously affect the emission line formation and therefore the parameters of WR stars may need reexamination. As compared to smooth wind models the same line fluxes can be obtained with higher stellar temperatures and smaller mass loss rates.

Multilevel non-LTE codes for the modelling of WR emission line spectra and continua have been developed for hot expanding atmospheres by Hillier (1987, 1989), Hamann & Schmutz (1987), Schmutz et al. (1989) and Koesterke et al. (1992). These models, treating line and continuum formation simultaneously, use the comoving frame formulation. These are the so-called "standard models" which assume spherical symmetry, homogeneity, radiative thermal balance and a fixed velocity law in the form:

$$v = v_0 + (v_\infty - v_0)\left(1 - \frac{R_*}{r}\right)^\beta \qquad (18)$$

with β being close to unity.

Nugis (1990a, 1990b) has developed empirical modelling routines to study the line emission and continuum formation in the spherically symmetric smooth winds of WR stars. According to this code, inner optically thick layers of the envelope are not treated at all. The effective stellar radius and temperature are found from the UV continuum fluxes and the velocity at that level is derived from the demand that for the adopted velocity law the theoretical line fluxes of He II would be equal to the observed values. Line radiation transfer was treated using the Sobolev method as formulated by Castor (1970). Continuum and line formation were studied separately, only when solving the statistical equilibrium equations for level populations numbers of He II for the first two series continua, the nontransparency of the envelope was treated by using the approximate scheme similar to that used by Castor & Van Blerkom (1970). The electron temperature in the envelope was found from the energy balance demand for free electrons. In the modelling study of Nugis (1990a) the velocity law was varied to achieve the best agreement with the observed data. To get agreement with the most prominent He II and He I line fluxes and IR/radio-fluxes it was necessary to assume that deceleration of the matter flow takes place starting from some distance in the wind and after that follows a zone of final acceleration.

In the present paper we will use for the modelling of He II, He I and H I line formation somewhat different empirical scheme which is applied both for the clumped and smooth wind models of the envelope. We assume throughout this paper that the wind velocity is well approximated by the standard velocity law (Eq.18) with β being unity. The effective stellar surface was adopted either to lie at the level where the wind velocity reaches the value equal to the local sound speed if the radial optical depth due to electron scattering of above-lying layers ($\tau_{\rm e}$) is less than 1.5, or if this is not the case, then to lie at the level from which $\tau_{\rm e} = 1.5$. The latter case corresponds approximately to the value of 2/3 for the averaged over wavelengths effective radial optical depth $\tau_{\rm eff} \approx \sqrt{\frac{3k}{k+\sigma}}(\tau_{\rm e} + \tau_{\rm abs})$ of the more or less plane-parallel photospheric region. The emergent stellar continuum flux in the UV spectral region, where $k_\nu^{\rm abs} \ll \sigma_{\rm T} N_{\rm e}$, can be expressed through the Planck function with the temperature at the level $\tau_{\rm eff} = 2/3$. We used the approximate solutions for continuum stellar flux and mean intensity (radiation density) derived for electron-scattering dominated opacity plane-parallel photospheres. By adopting for the deep photospheric layers the gray atmosphere temperature gradient (in scattering dominated opacity cases the real situation is nearing to this approximation), we will obtain the emergent stellar flux in the form (the formula (3.5) in the paper of Baschek et al. 1991):

$$\pi F_\nu \approx \left(T_{\rm eff}/T(\tau_{\rm eff} = 2/3)\right)^4 \pi B_\nu(T(\tau_{\rm eff} = 2/3)) \ . \qquad (19)$$

In the case of supernovae, studied by this approximation, the color temperature and effective temperature differ strongly, but in the case of WR stars the color temperature in the observable UV spectral range ought to be close to the effective temperature (according to our estimates). Throughout of this paper we will assume that $T_{\rm c}({\rm UV}) \approx T_{\rm eff} = T_*$. Of course, it is needed to take into account that at some wavelengths the wind (spherically symmetric envelope) is strongly contributing into the total flux (wavelengths lower than 911 Å and IR/radio wavelengths).

For wavelengths 911 Å $< \lambda <$ 100 000 Å, the mean continuum radiation densities (mean intensities) in the wind were found by the formula:

$$\rho_\nu(r) \approx W q_c \frac{f_\nu}{f_\nu^*} I_\nu^* \frac{4\pi}{c} \quad . \tag{20}$$

The intensity I_ν^* is equal to $B_\nu(T_*)$ and the ratios f_ν/f_ν^* were adopted to be $f_\nu/f_\nu^* = 1$ for 911 Å $<$ $\lambda \leq$ 2 000 Å and $f_\nu/f_\nu^* = (f_\nu I_\nu^*(2000))/(f_\nu(2000) I_\nu^*)$ for 2 000 Å $< \lambda <$ 100 000 Å. Here f_ν is the observed continuum flux and the factor q_c was estimated from the demand that for the range 911 Å $< \lambda \leq$ 2 000 Å the mean radiation density at the effective stellar surface would be equal to that of the plane-parallel scattering-dominated model atmosphere (we used the results of Baschek et al. 1991 and Hershkowitz et al. 1986). From this demand we will obtain $q_c = \sqrt{3}/2 \approx 0.866$ which follows from our estimate that $T_c({\rm UV}) \approx T_{\rm eff}$.

Continuum radiation densities for $\lambda \leq$ 911 Å were found by using somewhat modified version of the approximate solution of Castor & van Blerkom (1970):

$$\begin{aligned} \rho_\nu(r) \approx\ & W q_c \frac{I_\nu^* 4\pi}{c} e^{-t_\nu} + \\ & + W \frac{B_\nu(T_e) 4\pi \alpha_\nu^0}{c\alpha_\nu} \left(1 - e^{-t_\nu}\right) + \\ & + (1-W) \frac{B_\nu(T_e) 4\pi\alpha_\nu^0}{c\alpha_\nu} \left(1 - e^{-t'_\nu}\right) \quad , \end{aligned} \tag{21}$$

where $t'_\nu = \tau_\nu - t_\nu$, $t_\nu = \int_{R_*}^r \alpha_\nu dr$ and $\tau_\nu = \int_{R_*}^\infty \alpha_\nu dr$. Here $t_\nu = t_\nu^{\rm HI} + t_\nu^{\rm HeII} + t_\nu^{\rm HeI}$, whereas in absorption coefficients α_ν both b-f and f-f transitions are taken into account. For wavelengths where true absorption in the envelope is strong (τ is much greater than unity), the effective stellar surface lies well below the photosphere at respective wavelengths and here a good approximation to the stellar radiation density is $(4\pi\alpha_\nu^0 B_\nu(T_*))/(c\alpha_\nu)$ or when expressed in the form: $q_c 4\pi I_\nu^*/c$, we have that $q_c = 1$ and $I_\nu^* = (\alpha_\nu^0 B_\nu(T_*))/\alpha_\nu$, where α_ν^0 and α_ν are LTE and true absorption coefficients at $r = R_*$. For wavelengths 228 Å $< \lambda \leq$ 911 Å, q_c was found from the demand of continuity of radiation density at the effective stellar surface: $q_c = (\tau_\nu + \sqrt{3}/2)/(\tau_\nu + 1)$ and the intensity I_ν^* was adopted to be $B_\nu(T_*)$ if $\tau_\nu < 2/3$ and $(\alpha_\nu^0 B_\nu(T_*))/\alpha_\nu$ if $\tau_\nu \geq 2/3$.

For IR and radio wavelengths ($\lambda >$ 100 000 Å), the continuum radiation densities were obtained from iterative direct integration solutions (Eq. 42-44).

The stellar radius is found from the following relation:

$$\left(\frac{R_*}{d}\right)^2 = \frac{f_\nu 10^{0.4A_\nu}}{\pi B_\nu(T_*) q_\nu} \quad , \tag{22}$$

where $T_* = T_{\rm c}({\rm UV})$ and the factor q_ν considers the influence of the envelope. In the UV spectral region ($\lambda\lambda$1200 – 1500 Å), q_ν was found to be of the order of 0.75 (in the visual region $q_\nu \approx$ 1).

Density in the wind is obtained from radio fluxes. In the case of the spherically-symmetric smooth wind we have that:

$$\dot{M} = \frac{0.094}{\nu^{0.5}} \left[f_\nu({\rm Jy})\right]^{0.75} d^{1.5} v_\infty \frac{\mu}{\gamma^{1/2}\zeta^{1/2}} \quad , \tag{23}$$

where the mass loss rate is given in solar masses per year, the distance d in kpc, the terminal velocity v_∞ in km/s and μ is the mean molecular weight, γ is the mean number of electrons per ion and

$$\zeta = \sum_{A,z} x^+ g_{\rm ff}(A^{+z-1}) z^2 \quad , \quad x^+ = N^+(A^{+z-1})/N_{\rm tot} \quad .$$

From the mass loss rate we can determine the parameter:

$$N_\infty^*({\rm He}) = \frac{x_{\rm He}\dot{M}}{4\pi R_*^2 m_{\rm H} \mu v_\infty} \quad , \quad x_{\rm He} = N({\rm He})/N_{\rm tot} \quad . \tag{24}$$

The number density of helium atoms at some point in the smooth wind is equal to:

$$N_{\rm He}(r) = N_\infty^*({\rm He}) \frac{R_*^2 v_\infty}{r^2 v(r)} \quad . \tag{25}$$

For finding the number densities of helium atoms in the clumped wind, it is necessary to know the parameters of clumps at different distances.

The electron number density $N_{\rm e}(r)$ is obtained from the formula:

$$N_{\rm e} = N_{\rm He}\left(2\frac{N_{\rm He}^{++}}{N_{\rm He}} + \frac{N_{\rm He}^+}{N_{\rm He}} + \frac{N_{\rm H}}{N_{\rm He}} + \sum_{\rm CNO,z} \frac{z N_{\rm CNO}^{+z}}{N_{\rm He}}\right) . \tag{26}$$

Hydrogen remains in all cases predominantly ionized and helium ionization fractions are obtained from level population statistical equilibria equations. For finding the small contribution (especially in the case of WN stars) of CNO elements, it is needed to know their ionization state. The influence of C, N ions for WN stars and C, O ions for WC stars was found by adopting that at $r >$ 10 R_* the ionization state is one stage higher than the lowest ionization state of the observed non-resonance lines of these species in the spectrum and that at smaller distances the ionization state is one step higher.

The electron temperature in the envelope was found from the energy balance equation for free electrons to follow approximately the run:

$$\begin{aligned} T_{\rm e}(r) &= T_*(R_*/r)^{0.3} \quad \text{if } T_*(R_*/r)^{0.3} \geq T_{\rm e}^{\rm asym} \quad , \\ T_{\rm e}(r) &= T_{\rm e}^{\rm asym} \qquad\quad\ \text{if } T_*(R_*/r)^{0.3} < T_{\rm e}^{\rm asym} \quad , \end{aligned} \tag{27}$$

whereas $T_{\rm e}^{\rm asym}$ was estimated to lie in the range of 9 000 – 20 000 K for WN stars and in the range of 7 000–9 000 K for WC stars (earlier subtypes have higher values of $T_{\rm e}^{\rm asym}$). The influence of CNO ions is taken into account in finding the run of $T_{\rm e}$ (Nugis 1990b). The adopted temperature run is quite close to the detailed RE models of other authors. The helium and hydrogen line intensity ratios are not very sensitive to temperature and no serious errors ought to be introduced from this approximation.

The system of statistical equilibrium equations for finding level population numbers can be expressed in the form:

$$\frac{dN_k}{dt} = R_k + C_k = 0 \quad , \qquad k = 1, ..., k_0 \quad , \tag{28}$$

where R_k and C_k are the net rates of the population of the level k by radiative and collisional processes, and k_0 is the number of the last (the highest) treated level. The net collisional rate is equal to:

$$\begin{aligned} C_k \ = \ & \sum_{i=1}^{k-1}(N_i N_{\rm e} b_{ik} - N_{\rm k} N_{\rm e} a_{ki}) + \\ & + \sum_{j=k+1}^{k_{\rm o}}(N_j N_{\rm e} a_{jk} - N_{\rm k} N_{\rm e} b_{kj}) + \\ & + N_{\rm e}^2 N^+ a_{ck} - N_{\rm k} N_{\rm e} b_{kc} + \\ & + Cor_+^{\rm c}(k) - Cor_-^{\rm c}(k) \quad , \end{aligned} \tag{29}$$

where b_{ik}, a_{ik} are the collisional bound-bound excitation and de-excitation rates by electron impact, b_{kc}, a_{ck} are the collisional ionization and three-body recombination rates and $Cor^{\rm c}(k)$ are the correction terms which are described in the Appendix. The net radiative rate R_k can be written in the form:

$$\begin{aligned} R_k \ = \ & \sum_{j=k+1}^{k_{\rm o}}(N_j A_{jk} + N_j B_{jk}\langle\rho_{jk}\rangle - N_{\rm k} B_{kj}\langle\rho_{jk}\rangle) - \\ & - \sum_{i=1}^{k-1}(N_{\rm k} A_{ki} + N_{\rm k} B_{ki}\langle\rho_{ki}\rangle - N_i B_{ik}\langle\rho_{ki}\rangle) + \\ & + N_{\rm e} N^+ A_{ck} + N_{\rm e} N^+ B_{ck}\rho_{ck} - N_{\rm k} B_{kc}\rho_{kc} + \\ & + Cor_+^{\rm r}(k) - Cor_-^{\rm r}(k) \quad . \end{aligned} \tag{30}$$

In this formula A_{ki}, B_{ki} and B_{ik} are the Einstein coefficients of spontaneous and induced line emission and absorption. A_{ck} is the radiative spontaneous recombination rate, $B_{ck}\rho_{kc}$ and $B_{ck}\rho_{ck}$ are the photoionization and induced radiative recombination rates.

The numbers of photoionizations, induced and spontaneous radiative recombinations can be calculated by formulae:

$$N_{\rm k} B_{kc}\rho_{kc} \ = \ \int_{\nu_k}^{\infty} \frac{N_{\rm k}\kappa_\nu c\rho_\nu}{h\nu} d\nu \quad , \tag{31}$$

$$N_{\rm e} N^+ B_{ck}\rho_{ck} \ = \ N_{\rm e} N^+ z_k^\circ \int_{\nu_k}^{\infty} \frac{\kappa_\nu c\rho_\nu}{h\nu \exp(h\nu/kT_{\rm e})} d\nu \quad , \tag{32}$$

$$\begin{aligned} N_{\rm e} N^+ A_{ck} \ = \ & N_{\rm e} N^+ z_k^\circ \int_{\nu_k}^{\infty} \frac{\kappa_\nu 4\pi B_\nu(T_{\rm e})}{h\nu} \times \\ & \times \ (1 - \frac{1}{\exp(h\nu/kT_{\rm e})}) d\nu \quad , \end{aligned} \tag{33}$$

where κ_ν is the photoionization cross-section.

For He I dielectronic recombinations and radiative excitations from singly excited electronic states onto doubly excited states must be taken into account. The influence of dielectronic recombinations becomes substantial at high electron temperatures ($T_{\rm e} > 40\,000$ K, according to Ilmas & Nugis 1982). We consider only the most important dielectronic recombination processes involving radiative decay $2pnl \rightarrow 1snl$.

In calculating the integrated (over the local line profile) and averaged (over the angles) radiation densities ($\langle\rho_{ik}\rangle$) we used the Sobolev method (the line escape probability method). For the envelopes with non-decreasing velocity laws $v(r)$, we have (cf. Castor 1970) that:

$$< \rho_{ki} >= (1 - \beta_{ik}) S_{ki} + \beta_{ik}^{\rm c}\rho_{\rm c} \quad , \tag{34}$$

where β_{ik} is the escape probability coefficient, which is given by the formula:

$$\beta_{ik} = \int_0^1 \left[\frac{1 - {\rm e}^{[} - \tau_{ik}^0/(1 + \mu^2(dlnv/dlnr - 1))]}{\tau_{ik}^0/(1 + \mu^2(dlnv/dlnr - 1))}\right] d\mu \quad , \tag{35}$$

$$\tau_{ik}^0 \ = \ (\pi e^2/mc) g_i f_{ik} \lambda_{ik} (N_i/g_i - N_k/g_k) \frac{r}{v} \quad . \tag{36}$$

The line source function S_{ki} can be expressed as follows:

$$S_{ik} = \frac{N_{\rm k} A_{ki}}{N_i B_{ik} - N_{\rm k} A_{ki}} \quad . \tag{37}$$

In the study of Castor (1970) it was assumed that the optical depth of an envelope in the continuum spectrum is negligibly small at line frequencies. In such a case $\rho_{\rm c} \approx \rho_{\rm c}^*$ and $\beta_{ik}^{\rm c}$ is the probability that a photon escapes from the local region and strikes the star:

$$\beta_{ik}^{\rm c} = \frac{1}{2}\int_{\mu_{\rm c}}^1 \left[\frac{1 - \exp[-\tau_{ik}^0/(1 + \mu^2(dlnv/dlnr - 1))]}{\tau_{ik}^0/(1 + \mu^2(dlnv/dlnr - 1))}\right] d\mu, \tag{38}$$

$$\mu_{\rm c} \ = \ \sqrt{1 - (R_*/r)^2} \quad .$$

In our study we took into account also the continuous radiation of the envelope. We calculated the term $< \rho_{ki} >$ by the formula:

$$< \rho_{ki} >= (1 - \beta_{ik}) S_{ki} + \beta_{ik}^{\rm c}\rho_\nu^* \frac{f_\nu}{f_\nu^*} \quad . \tag{39}$$

At very long wavelengths, where envelope is optically thick, we have that:

$$< \rho_{ki} > \approx (1 - \beta_{ik}) S_{ki} + \beta_{ik} \frac{4\pi B_\nu(T_{\rm e})}{\rm c} \quad . \tag{40}$$

As all hydrogen lines (n, m) are slightly redshifted with respect to blending He II (i, k) lines $(n = i/2, m = k/2)$, in equations of statistical equilibrium for level populations of H I the dilution of the stellar continuum flux due to absorption by He II atoms lying closer to the stellar surface ($\nu_{ik}(s_1) = \nu_{nm}(s_2), s_1 < s_2$) must be taken into account. In addition the line radiation of neighboring blending He II atoms must also be considered. To calculate the population numbers of H I we used the following method: first we solved the equations of statistical equilibrium for level populations of He II at some r and then, at the same point, we solved the equations of statistical equilibrium for level populations of H I whereas radiation densities for H I transitions were found from the formula:

$$< \rho_{nm} > = (1-\beta_{nm})S_{nm} + \beta^{c}_{nm} e^{-\overline{\tau}^{\rm HeII}_{ik,c}} \rho_\nu + S^{\rm HeII}_{ki}(1-e^{-\overline{\tau}^{\rm HeII}_{ik}})\beta_{nm} \quad , \tag{41}$$

where

$$\overline{\tau}^{\rm HeII}_{ik} = \int_0^1 \frac{\tau^0_{ik}}{\mid 1+\sigma x^2 \mid} dx \quad ,$$

$$\overline{\tau}^{\rm HeII}_{ik,c} = \int_{x_c}^1 \frac{\tau^0_{ik}}{\mid 1+\sigma x^2 \mid} dx \quad , \quad x_c = \sqrt{1-\left(\frac{R_*}{r}\right)^2} \quad .$$

In level population statistical equilibria computations for He I we used the ionization fractions obtained from the solutions for He II+ H I.

Continuum fluxes at IR and radio wavelengths give us very valuable information about the reliability of the models used. These fluxes were found iteratively by direct numerical integration over the impact parameter ξ and the s-coordinate (along the line of sight):

$$F_\nu = 4\pi d^2 f_\nu 10^{0.4A_\nu} = 4\pi \int_0^{R_*} \left(I_\nu e^{-\tau_\nu(\xi)} + \int_0^{\tau_\nu(\xi)} S_\nu e^{-t_\nu} dt_\nu \right) 2\pi\xi d\xi + 4\pi \int_{R_*}^{\infty} \left(\int_0^{\tau_\nu(\xi)} S_\nu e^{-t_\nu} dt_\nu \right) 2\pi\xi d\xi \quad . \tag{42}$$

The inner boundary condition is that inward and outward intensities at stellar surface are equal to $B_\nu(T_*)$ and the upper boundary condition is that inward intensity is zero at infinity.

The source function for continuum radiation is equal to:

$$S_\nu = \frac{\alpha^\circ_\nu B_\nu(T_e) + N_e \sigma_T J_\nu}{\alpha_\nu + \sigma_T N_e} \tag{43}$$

and

$$J_\nu = \frac{1}{2r} \int_{-r}^{r} I_\nu(r, \sqrt{r^2-s^2}) ds \quad . \tag{44}$$

The intensities I_ν at different r, s values were found iteratively by adopting for the initial guess that $J_\nu = B_\nu(T_e(r))$. The whole envelope was divided into different zones of r and ξ, whereas inside different radial zones the mean values of T_e and v were used. In total 45 radial points and 52 ξ points were used (near the stellar surface a much denser set of r was used as compared to more distant regions where T_e and v are nearly constant). At IR and radio wavelengths the absorption coefficient is mainly due to free-free transitions. At IR wavelengths some small contribution is due to bound-free transitions and this may be considered adopting the Menzel coefficients b_k for the contributing high levels to be unity. Therefore, $\alpha_\nu = \alpha^\circ_\nu$. The electron scattering weakly influences the IR and radio fluxes which are effectively formed quite far (especially radio-fluxes) from the stellar surface. The optical depth $t_\nu(\xi)$ was found for a smooth wind case from the equation:

$$t_\nu(\xi) = \int_s^\infty N_e(\sum_{A,z} N^+ k_\nu + \sigma_T) ds \quad , \tag{45}$$

where

$$k_\nu(A^{+z}) = k^\circ_\nu z^2 (g_{\rm ff} + \frac{2z^2 I_H}{kT_e} \sum_{i=k}^{\infty} \frac{g_{i\nu}}{i^3} e^{\frac{I_i}{kT_e}}) \quad ,$$

$$\frac{I_k}{h} < \nu < \frac{I_{k-1}}{h} \quad ,$$

$$k^\circ_\nu = \frac{2^4 \pi^2 e^6 k T_e}{3\sqrt{3} ch (2\pi m_e k T_e)^{3/2} \nu^3} \left(1 - e^{-\frac{h\nu}{kT_e}}\right) \quad .$$

Here $g_{\rm ff}$ and $g_{i\nu}$ are the Gaunt factors for free-free and bound-free radiation, respectively, and σ_T is the Thompson scattering cross-section.

To get theoretical line fluxes, the dilution of the line emission due to electron scattering and continuum absorption by the above-lying layers of the envelope (factor f_c in Eq. (1)) must be considered. The factors f_c for every radial distance point were adopted to be the means of the blue and red parts of the line profile. The integrated mean factors f_c were estimated to lie in the range 0.5–0.9 for the lines with $\lambda \leq 3\ \mu$m. They are greater for IR optically thin high IP lines. It is difficult to consider this dilution correctly (for integrated line fluxes). To get reliable abundance ratios, the lines having close wavelengths must be used.

4. The clumped (ragged) wind model

Density condensations (clumps) of comparatively small contrast ($p \approx 1.1-2$) in relation to the ambient wind matter are assumed to arise at the effective stellar surface (probably due to pulsations which according to the paper of Maeder (1985) seem to be present in WR stars). These matter condensations are proposed not to take part in the $1/r^2$ wind expansion (stretching) when moving away from the stellar surface. The matter density in the clumps is determined by the change of their size which is caused by the expansion of clumps with the speed which is close to the local sound speed. Such kind of clumps lead to different values of matter contrast and filling factor at different radial distances. In the present study the clumps are assumed not to be confined by some forces and in this case they expand with the mass-average speed:

$$v_{\rm cl} = v_s \frac{1}{\gamma} \sqrt{\frac{2\gamma}{(\gamma-1)}} \quad , \tag{46}$$

where γ is the adiabatic exponent ($\gamma = 5/3$) and v_s is the adiabatic sound speed. These clumps are assumed to have spherical shape and move according to the same velocity law as the interclump medium. Electron temperature in the clumps is also taken to be the same as in the interclump medium at the same distance. At the stellar surface all the clumps are assumed to have the same size (the same mean radius).

For the ragged wind model computations we need to specify the filling factor δ, the contrast $p = N^h/N^l$ (the ratio of total number density of matter in the clumps N^h and in the surrounding interclump medium N^l) and the mean size of clumps $r_{\rm cl}$ at the stellar surface. At every other point in the envelope these parameters can be found from the equations given below. The matter contrast p first increases with the increase of radial distance and starts to decrease after reaching the maximum value (the filling factor δ behaves in the opposite way). The enhancement effect of the clumped wind for IR and line fluxes depends on the value of the factor: $(p^2\delta + 1 - \delta)/(p\delta + 1 - \delta)^2$. Near the stellar surface this enhancement factor is close to unity and reaches great values with the increase of parameter p. The whole effect of the enhancement depends on the maximum value of the enhancement factor obtained in the wind and on the extent of the region in the wind where this enhancement factor has values higher than unity. Our computations showed that from three parameters, describing the clumped wind models (initial matter contrast, initial filling factor and the mean size of clumps at the stellar surface), the enhancement factor depends most strongly on the mean size of clumps at the stellar surface and less sensitively on the initial matter contrast. We studied the range p_0 = 1.1 - 2. About two times increase in p_0 leads to less than 50 per cent increase of IR and line fluxes. In the present study we adopted p_0 = 1.2. The parameters $r_0 = r_{\rm cl}(R_*)$ and $\delta_0 = \delta(R_*)$ are left to be free parameters. From the demand of continuity of the matter flux in the envelope we will obtain:

$$\begin{aligned}\dot{M} &= 4\pi r^2 \mu v(r) m_{\rm H}[N^l(r)p(r)\delta(r) + N^l(r)(1-\delta(r))] = \\ &= const \ ,\end{aligned} \tag{47}$$

where $N^l(r)$ is the total number density of matter in the interclump medium at the distance r. The total number density of helium atoms at distance r in the interclump medium is equal to $N^l_{\rm He}(r) = N^l(r)x_{\rm He}$. We are dealing with the conservative situation (no exchange of matter between clumps and interclump medium) and in this case both members on the right hand side of Eq. (47) must be the constants. From that demand we will get the relationship:

$$p(r) = p_0 \frac{\delta_0}{\delta(r)} \frac{(1-\delta(r))}{(1-\delta_0)} \ . \tag{48}$$

The volume of the clumps at the radial distance r can be calculated from the formula:

$$V_{\rm cl}(r) = \frac{4}{3}\pi\left[r_0 + \int_{R_*}^{r} \frac{v_{\rm cl}(T_{\rm e})}{v(r)} dr\right]^3 \ . \tag{49}$$

The filling factor $\delta(r)$ is defined as:

$$\delta(r) = n_{\rm cl}(r) V_{\rm cl}(r) \ , \tag{50}$$

where $n_{\rm cl}(r)$ is the number density of clumps (the number of clumps in unit volume) and $V_{\rm cl}(r)$ is the volume of the clump at the distance r. The equation of continuity for the number of clumps can be expressed as:

$$n_{\rm cl}(r) = n_{\rm cl}(R_*)\left(\frac{R_*}{r}\right)^2 \frac{v_0}{v(r)} \ , \tag{51}$$

where v_0 is the wind velocity at the stellar surface.

From Eqs. 50 and 51 we will obtain that:

$$\delta(r) = \delta_0 \left(\frac{R_*}{r}\right)^2 \frac{v_0}{v(r)} \frac{V_{\rm cl}(r)}{V_{\rm cl}(R_*)} \ . \tag{52}$$

The energy emitted in the line can be expressed for the clumped wind model in the form:

$$E_{ki} = \int_V f_{\rm c}\left(\delta I^h_{ki} + (1-\delta)I^l_{ki}\right)(1-W)dV \ , \tag{53}$$

where

$$I^h_{ki}(r) = N^h_k \beta^h_{ik} A_{ki} h\nu_{ik} \ , \quad I^l_{ki}(r) = N^l_k \beta^l_{ik} A_{ki} h\nu_{ik} \ .$$

The values of N^h_k, N^l_k, β^h_{ik} and β^l_{ki} are obtained from the solution of statistical equilibrium equations at every r, starting from stellar surface. Inside the clumps we used an approximation similar to Antokhin et al. (1992). The equations of level population statistical equilibrium for clumps were solved for one representative point using the escape probability method according to Boland & de Jong (1984). The representative point was chosen according to the demand that the pathlength from it to the surface of the clump would have the mean value among all points of the clump. The outer layers of the clumps are expanding with the speed equal to $3v_{\rm s}$ if the pressure of the interclump matter can be neglected.

The optical depths for clumps at line frequencies were determined by the equation:

$$\tau_{ik} = \frac{\pi e^2}{mc} g_i f_{ik} \lambda_{ik} \left(\frac{N_i}{g_i} - \frac{N_k}{g_k}\right) \frac{0.912 r_{\rm cl}(r)}{3v_{\rm s}(r)} \ . \tag{54}$$

The escape probability coefficients for clumps were found from the relationships:

$$\beta_{ik} = \frac{1}{\tau_{ik}}(1-\exp(-\tau_{ik})) \ , \quad \beta^{\rm c}_{ik} = W\beta_{ik} \ . \tag{55}$$

Full helium atom densities at some r were derived through the parameter $N^*_\infty({\rm He})$ (which was introduced above):

$$\begin{aligned} N^h_{\rm He} &= N^*_\infty({\rm He})\frac{v_\infty}{v(r)}\left(\frac{R_*}{r}\right)^2 \frac{p}{[p\delta + (1-\delta)]} \ , \\ N^l_{\rm He} &= N^*_\infty({\rm He})\frac{v_\infty}{v(r)}\left(\frac{R_*}{r}\right)^2 \frac{1}{[p\delta + (1-\delta)]} \ . \end{aligned} \tag{56}$$

In finding the radiation densities for H I transitions (Eq. 41), the contributions of clumps and interclump medium into $S_{\rm HeII}$ and $\tau_{\rm HeII}$ are considered as follows: $\tau_{\rm HeII} = \delta\tau^h + (1-\delta)\tau^l$ and

Table 1. The list of the studied stars. WR numbers are from the Catalogue of van der Hucht et al. (1981). Narrow-band monochromatic magnitudes v_m ($\lambda \approx 5160$ Å) are from Massey (1984) and Torres & Massey (1988). E_{B-V} values are given in the broad-band Johnson system

WR	Name	Sp	v_m	E_{B-V}
3	HD 9974	WN 3 + O 4	10.70	0.39
152	HD 211564	WN 3	11.69	0.59
128	HD 187282	WN 4	10.56	0.31
1	HD 4004	WN 5	10.54	0.85
6	HD 50896	WN 5	6.96	0.12
138	HD 193077	WN 5 + O	8.11	0.70
8	HD 62910	WN6/C	10.61	0.81
71	HD 143414	WN 6	10.30	0.32
85	HD 155603B	WN 6	10.61	0.96
115		WN 6	12.35	1.60
134	HD 191765	WN 6	8.24	0.53
136	HD 192163	WN 6	7.64	0.57
141	HD 193928	WN 6	10.14	1.23
153	HD 211853	WN 6 + O	9.08	0.65
12		WN 7	11.05	0.81
22	HD 92740	WN 7 + abs	6.45	0.30
55	HD 117688	WN 7	10.88	0.70
78	HD 151932	WN 7	6.62	0.50
120		WN 7	12.35	1.42
148	HD 197406	WN 7	10.46	0.76
155	HD 214419	WN 7 + O	8.74	0.64
158		WN 7	11.46	1.13
16	HD 86161	WN 8	8.52	0.54
40	HD 96548	WN 8	7.87	0.39
123	HD 177230	WN 8	11.27	0.79
124	209 BAC	WN 8	11.60	1.16
156		WN 8	11.10	1.23
108	HD E313846	WN 9	10.13	1.04
111	HD 165763	WC 5	8.41	0.29
135	HD 192103	WC 8	8.50	0.37

$S_{\rm HeII}(1 - e^{-\tau_{\rm HeII}}) = \delta S^h(1 - e^{-\tau^h}) + (1 - \delta)S^l(1 - e^{-\tau^l})$. Far from the stellar surface where the wind velocity differs less than the local sound speed from the terminal value, for clumps the additional dilution of stellar radiation caused by the absorption in the interclump medium and in the clumps lying in the velocity interval $v(r) - v_s$ must be considered:

$$f_c^{\rm add} = \delta_{\rm eff}\exp(-\overline{\tau}^h_{ik}) + (1 - \delta_{\rm eff})(1 - \exp(-\overline{\tau}^l_{ik})) \ , \qquad (57)$$

where $\overline{\tau}_{ik}$ is calculated at the distance $v_\infty - v(r) = v_s$ and $\delta_{\rm eff} = (r - r_c)/2r_{\rm cl}$ (r_c is the point where $v(r) = v_\infty - v_s$) or $\delta_{\rm eff}$ is taken to be unity if $(r - r_c)/2r_{\rm cl} \geq 1$. The neglect of this additional dilution may overestimate the degree of ionization in distant clumps.

The continuum fluxes for the ragged wind models were found by Eq. (42), whereas the optical depths along the line of sight at different impact parameters were computed using

Table 2. The adopted mean values of intrinsic monochromatic colors $(b - v)_0$ and absolute visual magnitudes M_v

Subclass	$(b - v)_0$	M_v	Source for M_v
WN 3	-0.35	-3.9	mean of (1) and (2)
WN 4	-0.28	-4.2	(3)
WN 4.5	-0.25	-4.2	mean of (1) and (2)
WN 5	-0.25	-4.5	our estimate for WR 1
WN 6	-0.20	-5.5	mean of (1) and (2)
WN 7	-0.20	-6.5	(1)
WN 8	-0.15	-6.5	our estimate for WR 105
WC 5	-0.32	-3.7	(2)
WC 6	-0.32	-3.7	(2)
WC 7	-0.30	-4.8	(2)
WC 8	-0.30	-4.8	(2)
WC 9	-0.25	-4.8	(2)

(1) - Lundström & Stenholm 1984, (2) - van der Hucht et al. 1988, (3) - Breysacher 1986.

the formula:

$$t_\nu(\xi) = \int_s^\infty \left[\delta N_e^h(\sum_{A,z} N_h^+ k_\nu + \sigma_T) + \right.$$
$$\left. + \ (1 - \delta)N_e^l(\sum_{A,z} N_l^+ k_\nu + \sigma_T)\right] ds \ . \qquad (58)$$

5. Observational data

To determine of the hydrogen-to-helium ratios it is necessary to know the observational fluxes of He II, He I and H I lines. The equivalent widths of the emission lines must be corrected for the influence of the violet-shifted absorption. Usually such corrections make equivalent widths of emission lines 1.0 ~ 1.2 times higher and only in the case of the late type WN stars this correction factor may reach 1.5. We used the corrected EW from the Atlas of Smith & Kuhi (1981). For the stars not presented in the Atlas, this correction was neglected.

We analyze the He II and He II + H I lines over a wide spectral range from UV to IR and therefore the continuum energy distribution must be correctly determined. We use the lines with $\lambda > 2500$ Å and for that region the mean IS extinction curve determined by Seaton (1979) (UV range) and Sapar & Kuusik (1978) (optical and IR ranges) was adopted. The data about W_λ for He II, He I and H I for 30 WR stars were collected from different sources. The mean values of W_λ were used for every star if more than one reliable estimate were available. The mean values of W_λ together with the data sources are presented in Tables 6-13 (for WC stars also the dereddened line fluxes are given). The continuum energy runs for the studied stars were determined using the data from different sources, whereas the preference was given to the spectrophotometric data. For the stars with no reliable spectrophotometric measurements, we used the monochromatic magnitudes u, b, v, r from Torres & Massey (1988) and Massey (1984). The IUE low resolution archive spectra were used to determine the continuum runs in the UV spectral region. IR continua were calculated from the broad-band J, H, K, L photometric data of Pitault et al. (1983), Williams et al. (1987) and Williams & Antonopoulou (1981), whereas corrections for the removal of the line contribution in IR bands were performed according to Pitault et al. (1983).

Spectrophotometric data of Kuhi (1966) in the range $\lambda\lambda$3320 - 11 000 Å yield the basic information about continua for most of the studied stars in that spectral region. From these data the points least contaminated by lines were selected according to Cohen et al. (1975) and they were corrected to take into account the Vega calibration by Hayes & Latham (1975). To obtain the absolute fluxes, the continuum level at 5160 Å was adopted to have the monochromatic $v_{\rm m}$ value, whereas $f_\nu(v_{\rm m} = 0) \approx 3500$ Jy. In the range of $\lambda\lambda$8 000 - 11 000 Å we used the spectrophotometric data from Cohen et al. (1975) (for stars in common with Kuhi (1966) the mean continuum runs were used). The original data of Cohen et al. (1975) were corrected by $\Delta m = 0.17$ to transform them into the same average values of Kuhi (1966). For HD 96548 and 92740 the spectrophotometric observations of Hua et al. (1983) were used (to the continuum level at λ5160 the $v_{\rm m}$ magnitudes were assigned). For WR 12 (WN 7) and WR 120 (WN 7) the relative continuum runs were assumed to be equal to that of HD 151932 (WR 78) and the absolute level was adopted to correspond to the actual $v_{\rm m}$ magnitude for these stars. The same approach was used in the case of WR 115 (WN 6) and WR 8 (WN 6/C): for them the relative continuum run was adopted to be equal to that of HD 192163 (WR 136). Radio fluxes and far IR fluxes needed for our modelling study were taken from Hogg (1989), Abbott et al. (1986), IRAS Point Source Catalog (1985) and from Leitherer & Robert (1991) (fluxes at 1.3 mm). The observed broad band IRAS fluxes were transformed into monochromatic fluxes at central wavelengths of the respective bands by using the color corrections according to Beichmann et al. (1985). For normal IR continua (with no dust emission) the monochromatic fluxes are approximately 1.21, 1.195, 1.12 and 1.03 times lower as compared to the observed broad band values of 12, 25, 60 and 100 μm, respectively.

To transform the observed continuum fluxes into the dereddened fluxes we must know the $E_{\rm B-V}$ values for the studied stars. Recently, several new studies have been undertaken to determine the values of $E_{\rm B-V}$ for a wide sample of WR stars. The most frequently used method is that based on the nullifying of the 2200 Å bump, with different modifications making it less user-dependent, but unfortunately different authors still obtain quite different results. Vacca & Torres-Dodgen (1990) applied a new scheme for the nullifying of the 2200 bump and determined the color excesses for 44 galactic and 32 LMC WR stars (using low resolution IUE archive spectra). They assumed that the intrinsic continuum of WR stars can be represented by a power law $F_\lambda = \lambda^{-\alpha}$. In our further study an equal weight is given to different individual estimates of $E_{\rm B-V}$ by nullifying the 2200 bump in deriving the $E_{\rm B-V}$ (2200), whereas the finally adopted $E_{\rm B-V}$ was taken to be the mean of the estimates by different methods as described below. Schmutz & Vacca (1991) proposed a new method to derive the $E_{\rm B-V}$ values for WN stars based on "standard model" predicted relationships between the intrinsic color excesses and the continuum jump at 3645 Å. This new method is model-dependent and seems to give quite reliable estimates of $E_{\rm B-V}$ for WN 7-8 stars. Conti & Morris (1990) used the method of the intrinsic flux ratio of two He II lines λ1640 and λ4686 to determine $E_{\rm B-V}$ values, whereas the intrinsic flux ratio of these lines was found to be 7.6 as derived from the study of LMC WN stars. This method seems to give quite good estimates of $E_{\rm B-V}$ for early type WN stars (single and binary WN 6 and earlier subclasses). For late type WN stars their values of $E_{\rm B-V}$ seem to be overestimates. In addition to mean $E^{2200}_{\rm B-V}$, $E^{\rm SV}_{\rm B-V}$ (Schmutz & Vacca 1991) and $E^{\rm CM}_{\rm B-V}$ (Conti & Morris 1990) we used for single WN stars (WN 5 and later subtypes) the original estimates of color excesses by Smith (1968b) ($E^{\rm S68}_{\rm B-V}$) obtained assuming that the narrow band intrinsic photometric colors of Galactic and LMC WN stars are the same. Finally, we derived for all the studied WR stars an additional estimate of $E_{\rm B-V}$ by making use of the average intrinsic colors presented in Table 2 (they were estimated by us on the basis of the comparison with the results obtained by other methods). We used the monochromatic $(b-v)_{\rm m}$ values from Massey (1984) and Torres & Massey (1988) ($E_{\rm B-V} \approx 1.24[(b-v)_{\rm m} - (b-v)_0]$. In the case of WR stars for which monochromatic colors were not measured by these authors, we used the transformation relationships between the synthetic colors and monochromatic colors according to Torres & Massey (1988), whereas different photometric narrow-band observations were transformed into a standard system, using the relationships derived by Schmutz & Vacca (1991). Summing up, we determined the $\overline{E}_{\rm B-V}$ values as the means of different methods by the following scheme:

$$\overline{E}_{\rm B-V} = \overline{E^{2200}_{\rm B-V} + E^{\rm CM}_{\rm B-V} + E^{(b-v)_o}_{\rm B-V}}\,, \qquad \text{WN 3 - 4.5}$$

$$\overline{E}_{\rm B-V} = \overline{E^{2200}_{\rm B-V} + E^{(b-v)_o}_{\rm B-V} + E^{\rm CM}_{\rm B-V} + E^{\rm S68}_{\rm B-V}}\,, \qquad \text{WN 5 - 6}$$

$$\overline{E}_{\rm B-V} = \overline{E^{2200}_{\rm B-V} + E^{(b-v)_o}_{\rm B-V} + E^{\rm SV}_{\rm B-V} + E^{\rm S68}_{\rm B-V}}\,, \qquad \text{WN 7 - 9}$$

$$\overline{E}_{\rm B-V} = \overline{E^{2200}_{\rm B-V} + E^{(b-v)_o}_{\rm B-V}}\,, \qquad \text{WC stars}$$

6. Modelling study of some representative stars of different WR subtypes

Using the routines described in Sect. 3 we first made computations for the smooth wind models. The computations were made by scaling the density in the envelope through the observed values of radio fluxes (Eq.24). We found that with the ionization fractions obtained from the solution of the statistical equations for level populations of He II + H I (chemical compositions were taken from Nugis (1991) and terminal velocities from Prinja et al. 1990), the IR fluxes remain about 2 times lower as compared

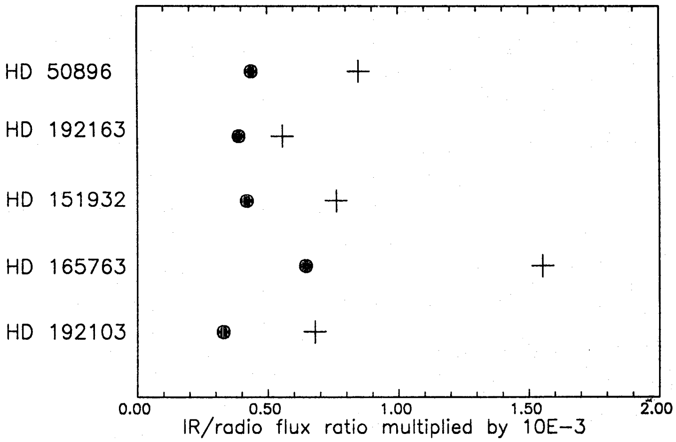

Fig. 3. The observed IR/radio fluxes (dots) in comparison with the smooth wind predictions (crosses). 4.9 GHz and 12 μm (10 μm for HD 192103 - WR 135 and HD 165763 - WR 111) fluxes were used. The model predicted IR fluxes were found by scaling the density in the envelope through the radio fluxes. We see that the smooth wind predicted IR/radio flux ratios remain about two times lower as compared to the observed values

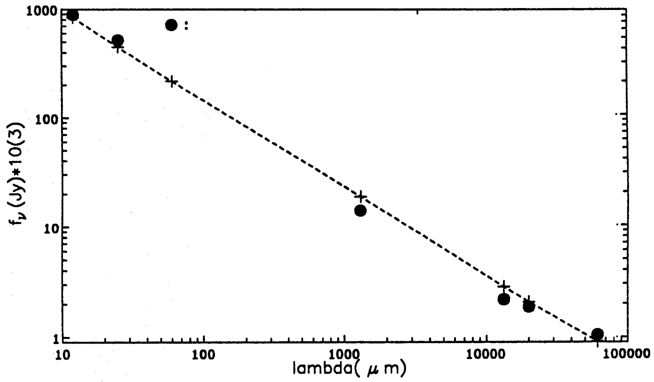

Fig. 4. The observed IR/radio fluxes of HD 50896 - WR 6 (dots) in comparison with the clumped wind model prediction (crosses)

to the observed fluxes for the studied stars (Fig. 3). Therefore the standard velocity law does not agree with the observational data on IR/radio fluxes and in our further study we will use the artificially increased density models for the smooth wind analysis. We used for all studied stars 1.5 times higher densities as compared to the densities derived directly from the observed values of radio fluxes. Such wind models assume that somewhere far from the stellar surface the velocity of matter flow increases 1.5 times over the value of v_∞. It is known that there exists a serious momentum problem for WR winds (the mass loss rates derived from radio fluxes exceed in some cases 30-50 times the single scattering limit $L/c/v_\infty$). Therefore, the increased density smooth wind models make this problem even more complicated. For WN 5 - 6 and WN 8 stars it was possible to obtain by these increased density smooth wind models quite good agreement with the line fluxes. In the case of WN 3 - 4 stars the He I line fluxes remained much weaker as compared to the observed fluxes.

In the case of HD 96548, when using the density parameter N^*_∞(He) derived from 25 μm flux value, we got reasonable agreement with the observed line fluxes. With this "IR density" the effective stellar surface ($\tau_c^{\rm env}$ = 1.5) occurs at quite high velocity value ($v_0 \approx 0.7 - 0.8 v_\infty$), but in the spectra of WN 8 stars we are observing absorption components at much smaller velocities. The contribution from the layers lying below the level $\tau_c^{\rm env}$ = 1.5 ought to be strongly suppressed by the continuum absorption and electron scattering and therefore this smooth wind model is problematical.

The difficulties (discrepancies) which appeared in the case of smooth wind models were not met in the clumped wind models. Figure 4 presents the observed IR/radio continuum spectrum of HD 50896 in comparison with the clumped wind model prediction. The agreement is quite good. In the case of HD 151932 the clumped wind model predicts somewhat higher than the observed flux at 1.3 mm. Radio emission region of WN 5 - 6 stars is practically not influenced by clumps (the matter contrast becomes nearly unity in this region). In the case of WN 7 - 9 stars the best agreement with the IR/radio fluxes and He II and He I line fluxes was obtained with larger clumps which retain substantial contrast in the effective radio-emission region, i.e radio fluxes of these stars are influenced by clumps. The clumps are strongly influencing also the formation of radio fluxes of WC stars.

Summing up, the clumped wind models seem to explain well main specific features of WN stars. The derived lower mass loss rates for WN stars can now be better explained by radiation driving only. For most subtypes of WN stars we have $\dot M/\dot M_1 \approx 1 - 3$, where $\dot M_1$ is the theoretical mass loss rate for the single scattering limit $\dot M_1 = L/c/v_\infty$. Only for WN 5 - 6 and WC stars this ratio achieves the values of 10-25.

7. Hydrogen–to–helium ratio

Our final aim was to derive as accurate as possible hydrogen-to-helium ratios for a large sample of WN stars and to find out whether there are some signs of the presence of hydrogen in the winds of WC stars.

The theoretical basis of our study are the clumped wind models and the smooth wind models with artificially increased densities (WN 5, WN 6 and WN 8 stars). The computations were made with the model parameters given in Table 3 and by the scheme described in Sects. 3-4. In the computations we used the 40 (He II), 20 (H I) and 52 (He I) level atom models, whereas the influence of higher levels was calculated via the scheme described in the Appendix. For late type WN stars (WN 7 - 9) it is important to include a large number of levels of He II otherwise it is not possible to consider correctly the contribution from the layers where helium is not predominantly doubly ionized.

Before making concrete determinations it is important to stress that many He II and He II + H I lines in the spectra of WR stars are seriously blended with the lines of other ions. Therefore, the choice of lines suitable for chemical composition studies is essential for getting reliable results. Let us point here

Table 3. The parameters of the clumped winds of our standard stars. Mean chemical compositions for the subclass have been used

WR	Sp	$d^{(2)}$ [kpc]	v_∞ [km/s]	T_* [K]	R_* [$R_\odot$]	N(H)/N(He)	$\dot{M}_{\rm cl}$ [$10^{-5}M_\odot/yr$]	$r_0^{\rm cl}$ [R_*]	δ_0
3[(1)]	WN 3 + O 4	7.12 (M)	3 100	90 000	3.16	0.1	1.03	0.035	0.3
128	WN 4	5.49 (M)	2 270	80 000	3.65	0.2	1.00	0.035	0.3
6	WN 5	1.62 (M)	1 720	50 000	6.14	0.2	3.53	0.035	0.3
				55 000	5.49	0.2	4.23	0.035	0.3
136	WN 6	1.82 (a)	1 605	45 000	11.15	0.3	7.00	0.030	0.3
				50 000	9.77	0.3	7.10	0.035	0.3
78	WN 7	2.00 (a)	1 365	38 000	18.97	0.5	2.50	0.035	0.4
40	WN 8	4.05 (M)	975	33 000	20.28	0.7	5.48	0.050	0.5
111	WC 5	1.58 (a)	2 415	55 000	4.00	0.0	1.68	0.012	0.3
135	WC 8	2.09 (a)	1 405	40 000	6.26	0.0	2.02	0.030	0.3

Comments: (1) - this star is a binary and from the comparison with the equivalent widths of HD 211564 (WN 3) we estimated that in the v - band WN 3 component contributes 40 % of the total flux.
(2) - information about the distance is given in brackets: (a) means that the star is a member of some association or open cluster and (M) that the distance is determined from the value of absolute visual magnitude according to Table 2
The mean contrast of matter at the effective stellar surface was taken to be 1.2 for all cases. For the stars with two models presented, the lower temperature model was used in final analysis.

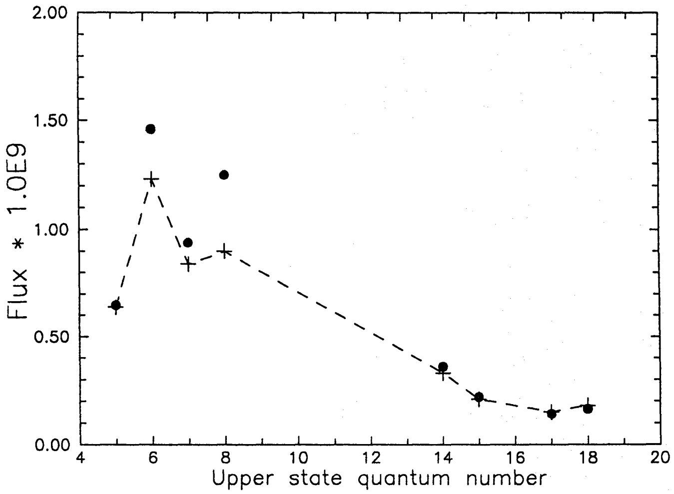

Fig. 5. The observed He II and He II + H I line fluxes of the star HD 192163 (WN 6) (dots) in comparison with the fluxes predicted by the clumped wind model (N(H)/N(He) = 0.6 and the other parameters are the same as in Table 3) (crosses). The model-predicted fluxes are joined by the smooth line. We see that the line λ4860 (8-4) is much stronger than the model predicted flux and as the other He II + H I lines agree quite well, the extra flux ought to be due to N III. The excess flux in λ4860 is seen also in the spectra of WN 7 - 9 stars

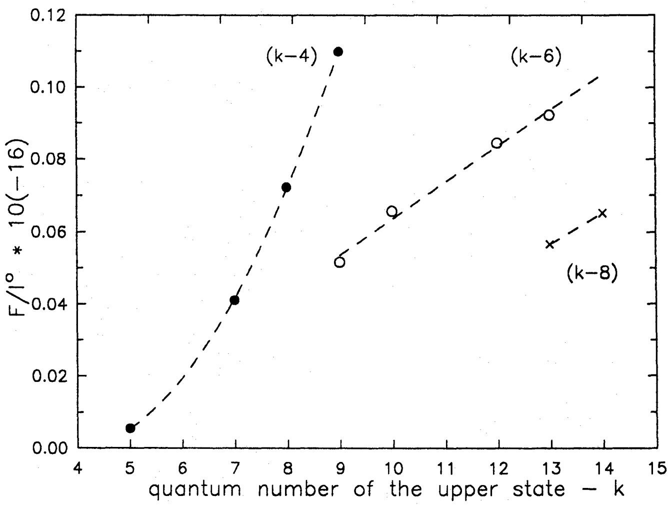

Fig. 6. The observed fluxes of weakly blended He II lines of (n − 4), (n − 6) and (n − 8) series of the star HD 192103 (WC 8). The observed fluxes are divided by the He II line intensity I_{ki}^0 at $T_{\rm e}$ = $T_*/2$. From the IR lines the contribution of He I is removed (Eenens & Williams 1992). We see that the decrement runs do not show the presence of H I

to some evidently blended lines, which, while used, may cause serious errors in the H/He ratio determination:

- λ3968 (He II (14-4), H I (7-2)) is in WNL stars blended with He I $4p^1P^0 - 2s^1S$,
- λ4100 (He II (12-4), H I (6-2)) is strongly blended with N III and Si IV lines in WN stars,
- λ4200 (He II (11-4)) is blended with N III and weakly with Si IV in WNL stars, whereas in WNE stars some additional contribution may come from S VI $5d^2D - 5p^2P^0$ transition,
- λ4340 (He II (10-4), H I (5-2)) is blended in WNL stars with N III whereas in WNE stars it is blended with N V $7p^2P^0 - 6s^2S$,
- λ4542 He II (9-4) is blended with N III, N IV lines in WN stars,

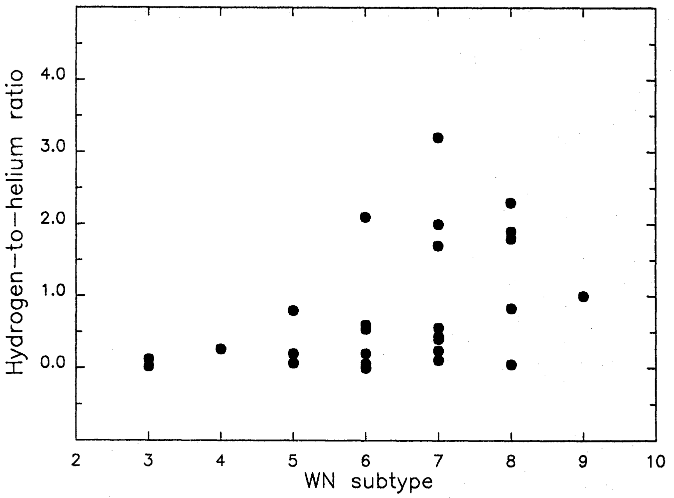

Fig. 7. The hydrogen-to-helium ratio as a function of the spectral subtype of WN stars. The increase of $N(\mathrm{H})/N(\mathrm{He})$ ratio with the spectral subtype is evident, the scatter is larger in later subtypes, however

- λ4860 (He II (8-4), H I (4-2)) is in WNL stars blended with N III
- the higher members of the series He II $(n-6)$, H I $(n-3)$ are blended with He I lines.

The least blended He II and He II + H I Pickering series lines in the spectra of WN stars are $\lambda\lambda$3924, 3968 (except WNL), 4860 (except WNL), 5411, 6560 and 10124. From the He II $(n-6)$ series lines the contribution of He I must be removed before using them for composition analysis (especially in the case of WNL stars). In the spectra of WC stars the higher Pickering series lines are practically all blended with lines of different ions of oxygen and carbon. In WCE spectra the lines $\lambda\lambda$4860 and 5411 are weakly blended and may be used for chemical composition determinations but in WCL stars these lines are also blended. Probably only the IR He II lines may be used for hydrogen-to-helium ratio determinations for WCL stars.

Let us now derive a formula for the determination of $N(\mathrm{H})/N(\mathrm{He})$ ratios. In the case of WN 7 and earlier WN stars, helium is doubly ionized up to some distance and then follows the zone where the ionization state of helium smoothly changes into the singly ionized state. For these stars we may express the line fluxes of the He II, He I and H I by formulae:

$$F_{\mathrm{HeII}} \propto \overline{b\beta_{\mathrm{HeII}}} I^0_{\mathrm{HeII}} \left(\int_{V1} N_e N(\mathrm{He}) dV + \right. \tag{59}$$

$$\left. + \; x \int_{V2} N_e N(\mathrm{He}) dV \right) ,$$

$$F_{\mathrm{HI}} \propto \overline{b\beta_{\mathrm{HI}}} I^0_{\mathrm{HI}} \frac{N(\mathrm{H})}{N(\mathrm{He})} \left(\int_{V1} N_e N(\mathrm{He}) dV + \right.$$

$$\left. + \int_{V2} N_e N(\mathrm{He}) dV \right) ,$$

$$F_{\mathrm{HeI}} \propto \overline{b\beta_{\mathrm{HeI}}} I^0_{\mathrm{HeI}} (1-x) \int_{V2} N_e N(\mathrm{He}) dV ,$$

Table 4. The parameters a_1, b_1, c_1 and d_1 of some selected line pairs found for clumped wind models with the H/He ratios presented in Table 3. From He Ilines λ 5876 is used for WN 5 and later subtypes and λ 10830 is used for WN 3 - 4 stars

λ of F_{bl} and F_{HeII}	a_1	b_1	c_1	d_1
WN3				
3968/3924	1.04	0.0041	1.66	0.0035
4859/5412	0.77	0.0	1.53	0.0085
10938/10426	1.04	0.0074	3.56	0.0020
WN4				
3968/3924	1.01	0.0061	1.33	0.0042
4859/5412	0.80	0.0	1.25	0.0099
10938/10426	1.04	0.011	3.26	0.0027
WN5				
3968/3924	0.98	0.052	1.21	0.047
10938/10426	1.06	0.058	3.35	0.035
8756/8706	1.11	0.0065	1.34	0.0044
WN6				
3968/3924	0.99	0.027	1.06	0.033
10938/10426	1.10	0.034	2.26	0.021
8756/8706	1.12	0.0039	1.19	0.0028
WN7				
3968/3924	0.87	0.076	0.95	0.027
10938/10426	1.08	0.056	6.30	0.044
8756/8706	1.15	0.0066	2.10	0.0054
WN8				
3968/3924	0.78	0.16	0.81	0.044
10938/10426	1.05	0.076	6.94	0.085
8756/8706	1.15	0.010	1.92	0.011

where I^0 is the reduced line intensity defined in Sect. 2, and the mean values of coefficients $\overline{b\beta}$ are derived from the integrated theoretical line fluxes found by the modelling study.

In the present paper we used the value $T_e = T_*/2$ which ought to be close to the mean value of T_e in the envelope. In the case of WN 8 - 9 stars, helium is only partly ionized near the stellar surface and very quickly the zone is reached where helium is singly ionized. For these stars the line fluxes may be written down by formulae:

$$F_{\mathrm{HeII}} \propto \overline{b\beta_{\mathrm{HeII}}} I^0_{\mathrm{HeII}} x \int_{V1} N_e N(\mathrm{He}) dV , \tag{60}$$

$$F_{\mathrm{HI}} \propto \overline{b\beta_{\mathrm{HI}}} I^0_{\mathrm{HI}} \frac{N(\mathrm{H})}{N(\mathrm{He})} \left(\int_{V1} N_e N(\mathrm{He}) dV + \right.$$

$$\left. + \int_{V2} N_e N(\mathrm{He}) dV \right) ,$$

$$F_{\mathrm{HeI}} \propto \overline{b\beta_{\mathrm{HeI}}} I^0_{\mathrm{HeI}} \left((1-x) \int_{V1} N_{\mathrm{e}} N(\mathrm{He}) dV + \right.$$
$$\left. + \int_{V2} N_{\mathrm{e}} N(\mathrm{He}) dV \right) .$$

F_{HI} is the hydrogen contribution in the blended line. To remove the contribution of He I and He II we must know the $\overline{b\beta}$ values for the blending line (1) and for some unblended line (2). For finding F_{HI} we can use the relationship:

$$F_{\mathrm{HI}} = F_{\mathrm{bl}} - \frac{(\overline{b\beta} I^0)^{(1)}_{\mathrm{HeII}} F^{(2)}_{\mathrm{HeII}}}{(\overline{b\beta} I^0)^{(2)}_{\mathrm{HeII}}} - \frac{(\overline{b\beta} I^0)^{(1)}_{\mathrm{HeI}} F^{(2)}_{\mathrm{HeI}}}{(\overline{b\beta} I^0)^{(2)}_{\mathrm{HeI}}} . \qquad (61)$$

The most reliable results ought to be obtained if the unblended lines lie near the blended lines. Then the factors f_{c} introduced in Sect. 2 cancel out and uncertainties in the continuum run are minimal. We used the He I line λ5876 (λ10830 for WN 3-4 stars) in H/He ratio determinations.

From the presented relationships we can derive the formula:

$$\frac{N(\mathrm{H})}{N(\mathrm{He})} = \frac{F_{\mathrm{bl}} - a_1 F_{\mathrm{HeII}} - b_1 F_{\mathrm{HeI}}}{c_1 F_{\mathrm{HeII}} + d_1 F_{\mathrm{HeI}}} . \qquad (62)$$

Let us now describe our method of determination of H/He ratios. For our standard stars (Table 3), we first adopted the mean abundance ratios of N(H)/N(He) for every sybtype as derived by Nugis (1991) and the ratio N(N)/N(He) = 0.003. With these abundances we found the model parameters which gave agreement with the observed He II and He I line fluxes and with the IR/radio fluxes for the standard stars.

From the theoretical line fluxes of the standard stars, we computed the parameters a_1, b_1, c_1, d_1 by using the Eqs. (59-62). The parameters a_1, b_1, c_1, d_1 presented in Table 4 correspond to the mean H/He values for the subclass. When using these parameters for some star of the same spectral subtype, we can estimate the "initial guess" value for H/He when putting into the Eq. (62) the observed line fluxes of that star. If the derived value of H/He differs less than two times from the used mean value for the standard star, then this ratio is adopted to be the final value for the N(H)/N(He) ratio. But if the "initial guess" value differs more than two times from the mean value, then the new model was computed for this subtype, retaining all the input parameters listed in Table 3 the same and changing only two times the H/He ratio. That is, we used for every subtype the grid of models with two times differing H/He ratios. This step is enough for getting the results which have "intrinsic preciseness" of the order of 10-20 %. When using the highest lines of $(n-6)$ series with $n > 20$, then already the "initial guess" values differ less than 10-20 % from the final results obtained with the corrected H/He ratio models. We checked that the H/He ratios found by using the individual models differ little from the results obtained with the models of the representative stars for the subtype (such comparison was made for WR 1, WR 134 and WR 156). The differences were less than the uncertainty limits of our method.

In the case of WN stars the best estimates of the hydrogen-to-helium ratio can be obtained from the neighboring He II $(n-6)$ series lines ($n \geq 12$). The contribution of He I in the He II + H I blends of this series is substantial some WN 8 stars (about 50% of the total flux) but in earlier subtype WN stars this contribution is quite small. Good estimates of hydrogen-to-helium ratio can be obtained also by comparing the line fluxes of the neighboring higher Pickering series lines ($n \geq 14$) (the contribution of He I must be removed from the blends). For hotter WN stars (WN 5 and earlier subtypes) quite reliable results can be obtained by using the lines λ5411 and λ4860. In later subtypes (WN 6 - 9) the line λ4860 is substantially blended with N III (see Fig. 5).

From our modelling study we can draw the conclusion that the envelopes of WN stars are optically thick in lower members of the Balmer series lines of hydrogen and therefore this must be taken into account in the determination of H/He ratios. Due to optical thickness of H I lines in the Balmer series, the He II contribution in the Pickering series blends He II + H I is suppressed and therefore by comparing the line fluxes of neighboring He II and He II + H I lines we may strongly underestimate the relative abundance of hydrogen if the line overlap effects are neglected. The results of our estimates of $N(\mathrm{H})/N(\mathrm{He})$ ratios obtained for 28 WN stars and 2 WC stars are given in Table 5. The presented $N(\mathrm{H})/N(\mathrm{He})$ ratios are the means of the estimates of different line pairs of higher members of the He II $(n-6)$ and $(n-4)$ series (in the case of WN 5 and earlier subtypes the lines 4860 and 5411 were also used in deriving the means). The errors of our estimates are about 30 % and in the case of the data presented with colons the errors reach 50-100 %. Our aim was to use such lines which can give us model-independent information on H/He ratios. We can conclude that more-or-less model-independent H/He ratios can be obtained for WN 3 - 7 stars when using the highest $(n-6)$ series lines ($n > 20$), but for WN 8 - 9 stars even these lines show some model-dependence (smooth wind model of the WN 8 star HD 96 548 yields the value $N(\mathrm{H})/N(\mathrm{He}) \approx 1.7$ which is about two times higher than the estimate obtained by the use of the clumped wind model). When using lower $(n-6)$ series lines ($n < 20$) or the Pickering series lines, the results remain somewhat model-dependent even for WN 3 - 7 stars (by smooth wind models we obtained for the stars HD 50 896 (WN 5) and HD 192 163 (WN 6) that $N(\mathrm{H})/N(\mathrm{He}) \approx 0.25$ and 0.45 respectively, whereas the clumped wind model estimates were 0.2: and 0.54).

Our new $N(\mathrm{H})/N(\mathrm{He})$ ratios agree qualitatively quite well with the "standard model" (smooth wind) results obtained through the Pickering series line profile studies by Hamann et al. (1994) and Crowther (1993).

Presented here $N(\mathrm{H})/N(\mathrm{He})$ ratios for common WN 3 - 6 stars agree well with the previous estimates based on the analysis of higher members of the Pickering or $(k-6)$ series lines (Nugis 1988; Vreux et al. 1989). Some differences with the results of Conti et al. (1983) who used intermediate Pickering series lines, are mainly due to blending effects. In the case of WN 7 - 9 stars, however substantial differences appear with the results of Conti et al. (1983) and Vreux et al. (1989, 1990). Their results must be regarded as upper limits of H/He ratios for WN 7 - 9 stars (ionization stratification effects were neglected in these studies).

Table 5. The hydrogen-to-helium ratios (by number) obtained by the use of clumped wind models. For binary stars (WR 3, 22, 138, 153, 155), the spectral type of the WR component is given only. Colons indicate the uncertain results of our estimates (the cases when only one pair of lines was used or when different lines gave strongly differing results)

Star	Sp	Previous results					This
WR		N88	CLP83	V89/90	C93	H94	study
3	WN 3 + O4	≤ 0.1	2.0			0.0	0.02:
152	WN 3		0.8		0.8	0.76	0.13
128	WN 4	0.22	0.4		0.5	1.0	0.26
1	WN 5		<0.2		<0.01	0.0	0.07:
6	WN 5	0.25	<0.1		<0.02	0.0	0.20:
138	WN 5 + O				0.3		0.8:
8	WN6/C				0.0		0.2:
71	WN 6		<0.1				0.6:
85	WN 6		0.6	2.0[1]			2.1
115	WN 6		<0.6			0.0	0.01:
134	WN 6	0.16	<0.1		<0.01	0.0	0.2:
136	WN 6	0.45	<0.3		0.3	0.55	0.54
141	WN 6				<0.01	0.0	0.0
153	WN 6 + O						0.06:
12	WN 7			5.0[1]		1.5	1.7
22	WN 7 + abs		4.0	5.0[1]	3.5	2.7	3.2
55	WN 7		<0.1			0.0	0.44
78	WN 7	0.31	1.0	1.5[1]	0.6	0.71	0.40
120	WN 7					0.0	0.11
148	WN 7		<0.3	1.0[2]		0.71	0.56
155	WN 7 + O			1.0[2]		0.0	0.24
158	WN 7		4.0	7.5[2]		1.7	2.0
16	WN 8		2.0	6.5[1]	1.0		1.8
40	WN 8	0.67	2.0	9.0[1]	1.0	0.71	0.83
123	WN 8		<0.4	1.0[2]	0.01	0.0	0.05:
124	WN 8			11.0[2]	0.6		1.9
156	WN 8	1.3	4.0	9.0[2]	1.5	1.7	2.3
108	WN 9		2.0		1.5		1.0
111	WC 5	$\leq$0.1					0.0
135	WC 8	$\leq$0.1					0.0

Comments: N88 - Nugis 1988, CLP83 - Conti et al. 1983, V89 - Vreux et al. 1989, V90 - Vreux et al. 1990, C93 - Crowther 1993, H94 - Hamann et al. 1994. [1] - refers to V89, [2] - refers to V90.

The hydrogen-to-helium ratio is in all studied WN stars lower than the mean cosmic ratio and in WC stars no hydrogen seems to be present (see Fig. 6). Hydrogen abundance is decreasing when going from WN 8 - 9 stars to WN 3 stars. Substantial intrinsic scatter seems to be present among the stars of the same subtype (the scatter is larger in later subtypes).

8. Concluding remarks and discussion

We found from the modelling study of some representative WR stars that good agreement with the observed He II, He I, H I line fluxes and with IR/radio fluxes can be obtained only in the case of the clumped wind model. Not to be strictly confined to one type of models we also performed the modelling study of the same standard WR stars with the smooth wind models assuming the standard velocity law (β = 1). With the densities derived directly from the observed values of radio fluxes it was not possible to reach agreement with the IR fluxes and line fluxes when using the smooth wind structure. With the increased density smooth wind models (i.e. scaling the density through the IR fluxes or He II line fluxes) we get wrong radio fluxes and for some subtypes also wrong He I line fluxes (WN 3 - 4). Our results for smooth wind models agree well with the "standard model" studies of Crowther (1993) and Hamann et al. (1991, 1994) for WN 5 - 7 stars, because their mass loss rates of the best fit smooth wind models are also about 1.5-2 times higher than the mass loss rates derived from the observed values of radio-fluxes. It is not easy to compare the stellar temperatures used in different modelling codes. The "standard model"

Table 6. Equivalent widths in Å. Code numbers of data sources (they are decoded at the end of Table 13) are given in the brackets. Uncertain data are indicated by colons

He II		WR1	WR 115	WR134	WR136
i	k	EW			
3	4	459(1,2)	112(2)	287(1,10)	302(12)
3	5	-	-	72(10)	84(11)
3	6	-	-	26.7(9)	35(9)
3	7	-	-	16.8(9)	18.5(9)
4	5	389(5,6)	124(6,7)	367(5,6)	293.2(6)
4	6	93(3)	36.2(8)	123(10)	161(8)
4	7	66(4)	18.0(8)	62(1,4)	56.6(8)
4	8	27(3)	11.1(8)	37(1,10)	52.9(1,8)
4	9	24.5(1)	10.0(8)	22(1)	36:(1,8)
4	10	20(1)	6.7(8)	24.2(1,10)	31.7(1,8)
4	14	5.6(1)	-	6.7(1,10)	7.9(1,11)
4	15	4.2(1)	-	3.8(1,10)	4.6(1,11)
4	17	2.1:(1)	-	2.0:(1,10)	2.8:(1)
4	18	2.9:(1)	-	2.3:(1)	3.2(1)
5	9	62(7)	18(7)	62(7)	54(7)
5	12	18(7)	7.4(7)	18(7)	18(7)
5	16	-	-	4.6(10)	6.1(11)
6	12	35:(6)	17.4(6)	24.5:(6)	37.8(6)
6	13	20.3(6)	10.6(6)	19.6(6)	14.3(6)
6	14	-	7.9(6)	20:(6)	13.1:(6)
6	15	13.7(6)	6.2(6)	15.3(6)	11.2(6)
He I					
5875		24(4)	11(8)	25(4)	26.5(4,12)
10830		358(5,6)	135(6)	280(5,6)	250.9(6)

Table 7. See the caption of Table 6

He II		WR8	WR138	WR141	WR153
i	k	EW			
3	4	114.4(13)	69.5(2,11)	74.5(1,2)	49.0(2,11)
3	5	24.4(13)	22.6(11)	-	11.9(11)
3	6	13.7(13)	-	-	-
3	7	6.4(13)	-	-	-
4	5	118(14)	95(5,6)	215(5,6)	84.8(5,6)
4	6	53.2(13,14)	45(8,11)	68.5(8)	-
4	7	27.4(13)	13.4(8,11)	37.0(5,8)	9.0(2)
4	8	21.7(13)	12.0(8,11)	19.7(1,8)	7.3:(11)
4	9	19.1(13)	6.0(8,11)	14.0(1)	4.9:(11)
4	10	13.4(13)	5.3(8,11)	10.8(1,8)	3.3(11)
4	14	4.2(13)	1.8(11)	2.5:(1)	0.5:(11)
4	15	3.0(13)	0.7(11)	2.9:(1)	0.3:(11)
4	17	1.4(13)	0.3(11)	0.9:(1)	0.3:(11)
5	9	34.7(14)	16.2(7)	28.2(7)	8.0(7)
5	12	4.4(14)	5.5(7)	10.2(7)	-
5	15	2.8(14)	2.7(11)	-	-
5	16	-	2.5(11)	-	-
6	12	-	14.3:(6)	17.4(6)	9.8(6)
6	13	-	5.6(6)	13.8(6)	4.2(6)
6	14	15.6(14)	6.1(6)	10.9:(6)	3.5(6)
6	15	-	4.3(6)	8.4(6)	1.9:(6)
He I					
5875		34.4(13,14)	5.2(11)	13(8)	-
10830		-	58.2(5,6)	142(5,6)	83.7(5,6)

code uses the core temperature which in most cases cannot be compared with the observed color temperature. We assumed in our empirical modelling study that continuum formation region in the observable UV spectral region $\lambda\lambda$1000-2000 Å is not very extended and that the relationships between the color and the effective temperature derived for plane-parallel scattering-dominated photospheres of hot stars (Baschek et al. 1991) are applicable for the UV continua of WR stars. Fortunately, in the case of WR stars the opacities due to Thompson scattering and true absorption are on the average related in such portion that T_c(UV)$\approx T_{\rm eff}$.

Our temperatures T_c(UV) $\approx T_*$ are intermediate between the "standard model" core temperatures and the temperatures at the level τ(Ross)= 2/3 and this shows that our empirical approach is physically quite reasonable. Most serious differences with our empirical models and the "standard models" may appear in the EUV continua. Crowther (1993) models predict for WN stars quite strong enhancement of the EUV flux, but the lines of iron group ions must strongly influence the flux in that range (Schmutz 1991). The enhanced EUV continuum flux may somewhat change the ionization structure of helium in the wind. When using the empirical modelling code this leads to lower stellar temperatures for getting the agreement with the observed fluxes of He II and He I lines. Our estimates showed that the uncertainties in the EUV continua lead to strong uncertainties in $T_{\rm eff}$ and L but the ratios of theoretical line fluxes of the neighboring higher lines of the Pickering and $(n-6)$ series remain nearly the same (nearly the same remain also the parameters a_1, b_1, c_1, d_1) and therefore the H/He ratios determined through these lines are not sensitive to the uncertainties in the EUV continuum spectrum. The uncertainties in the density structure of the wind may lead to about factor of two differences in the H/He ratios for WN 8 - 9 stars even when using the highest He II $(n-6)$ series lines.

Although our clumped wind models are a little schematic, on the basis of the present study we may conclude that such models enable us to explain the main specific features of the spectra of WR stars. The lower mass loss rates derived by clumped wind models (as compared to the "standard models" and our increased density smooth wind models) can now be better explained by radiation driving only. For most WN subtypes we got from the clumped wind models that mass loss rates are 1-3 times higher than the single scattering limit and only for WN 5 - 6 subtypes and WC stars the mass loss rates exceed 10-25 times this limit. Our aim of the present study was to estimate as precisely as possible the hydrogen-to-helium ratios for tens of WN stars. The modelling study performed in this paper was needed to find out the "best" He II, H I and He I lines which are not strongly depending on concrete details of the models. Our study showed that theoretical fluxes of He II + H I lines are quite seriously changed as compared to the case when the mutual influence of He II and H I is neglected in radiation transfer

Table 8. See the caption of Table 6

He II		WR3	WR6	WR128	WR152
i	k	EW			
3	4	53.0(2,11)	302(11)	98.5(11,12)	110(2)
3	5	3.2:(11)	90(9)	22.4(11)	-
3	6	-	29.0(9)	6.0(16)	-
3	7	-	20.0(9)	3.0(16)	-
4	5	124(5)	412(6,7)	173(5)	181(5,6)
4	6	28.8(8,11)	130(8)	74.7(11,12)	77.0(8)
4	7	7.5(4,8)	63.0(8,11)	17.5(4,12)	18.6(8)
4	8	4.1(11)	39.3(8,11)	13.4(11,12)	13.6(8)
4	9	3.2(11)	25:(11)	5.7(11)	5.0:(8)
4	10	1.8(11)	21.3(8,11)	5.2(11)	6.5(8)
4	13	-	-	1.4(11)	1.6(8)
4	14	0.9(11)	6.4(11)	1.2:(11)	-
4	15	-	4.0(11)	0.8:(11)	-
4	16	0.6(11)	-	1.2:(11)	-
4	17	-	1.7:(11)	0.4:(11)	-
5	9	-	46(7)	15.0(7)	15.5(7)
5	12	-	10.5(7)	4.5(7)	5.5(7)
5	13	-	23(7)	3.1(7,11)	3.1(7)
5	15	-	-	2.3(11)	-
5	16	-	-	1.8(11)	-
5	17	-	-	1.9(11)	-
5	18	-	-	1.0(11)	-
6	10	-	86.0(15)	-	-
6	12	-	40:(6)	-	13.5:(6)
6	13	-	19.9(6)	-	9.2(6)
6	14	-	5.2:(6)	-	8.8:(6)
6	15	-	9.0(6)	-	4.4(6)
7	10	-	165(15)	-	-
8	10	-	470(15)	-	-
8	13	-	77(15)	-	-
8	14	-	57(15)	-	-
8	15	-	45(15)	-	-
He I					
5876		-	21(8)	-	-
10830		-	326(4,6)	41(5)	15(5,6)

Table 9. See the caption of Table 6

He II		WR55	WR71	WR108	WR120
i	k	EW			
3	4	135(2)	150(2)	9.9(2)	79(2)
4	5	138(14)	156(7,14)	8.6(5,6)	73.2(6)
4	6	48.7(8,14)	53.7(14)	19.0(3)	35.7(6)
4	7	26.2(8)	30.0(2)	1.0(4)	17.2(8)
4	8	19.3(8)	14.7(17)	4.7(3)	14.3(8)
4	9	15:(8)	14.7(3,17)	1.1(3)	13.8(8)
4	10	9.0(8)	10.6(3,17)	2.2(3)	8.0(8)
4	14	-	3.8(17)	-	-
4	15	-	2.8(17)	-	-
5	9	21.0(7,14)	26.5(14)	-	17(7)
5	11	10.7(14)	13.1(14)	-	-
5	12	3.0(14)	9.3(14)	-	7.4(7)
5	15	3.0(14)	5.3:(17)	-	-
5	16	-	3.8:(17)	-	-
6	12	-	-	8.2:(6)	20.9(6)
6	13	-	-	-	7.0(6)
6	14	20.1(14)	17.8(14)	2.1(6,7)	13.3(6)
6	15	4.5(14)	3.7(14)	-	4.4(6)
6	21	0.60(14)	1.5(14)	-	-
6	22	1.9(14)	1.4(14)	-	-
He I					
5876		23.4(8,14)	12.3(14)	4.7(2,4)	23(2)
10830		-	-	43.5(5,6)	254.4(6)

Table 10. See the caption of Table 6

He II		WR12	WR123	WR124	WR148
i	k	EW			
3	4	72(2)	32.5(2)	37(2)	22.4(2)
4	5	59(7)	40.0(5)	22(5)	34(5)
4	6	107.0(8)	14.0(8)	91.7(8)	28.9(8)
4	7	11.4(8)	8.5(8)	4.0(8)	3.0(8)
4	8	26.1(8)	8.8(8)	27.7(8)	5.0(8)
4	9	9.5(8)	-	11.8(8)	4.4:(8)
4	10	17.0(8)	6.2(8)	16.9(8)	1.6:(8)
5	9	7.4(7)	13.0(7)	-	4.0(7)
5	12	-	4.8(7)	-	-
6	13	-	4.5(5)	2.8(5)	2.0(5)
6	14	27.0(18)	20.0(5)	32.0(5,7)	5.0(5)
6	15	2.6(18)	3.2(5)	2.2(5)	1.6(5)
6	22	6.2(18)	-	6.3(5)	0.90(5)
6	23	0.81(18)	0.63(5)	0.32(5)	0.20(5)
6	24	4.2(18)	1.8(5)	4.5(5)	0.63(5)
6	25	0.59(18)	0.71(5)	0.50(5)	0.20(5)
6	26	2.1(18)	1.4(5)	3.2(5)	0.30(5)
He I					
5876		23(8)	30(8)	46(8)	5.4(2)
10830		-	403(5)	373(5)	65(5)

treatments (especially in the case of WN 5 - 9 stars). The populations of H I are not strongly influenced by the suppression of stellar continuum radiation (due to absorption by blending He II atoms) and by line radiation of surrounding He II atoms but line radiation of He II is quite strongly suppressed (especially in the Pickering series) due to absorption caused by H I atoms lying in front of He II atoms (in relation to a distant observer). This suppression is quite substantial in the case of WN 7 - 9 stars and quite remarkable also in WN 5 - 6 stars. The He II $(n-6)$ series lines are only slightly influenced by this effect and they are better suited for determining the hydrogen-to-helium ratio in late type WN stars (H I second principal quantum number state is strongly overpopulated as compared to the third state).

From our modelling study we derived simple formulae which can be used for mass-estimates of hydrogen-to-helium ratios for WN stars. In the present study the H/He ratios were determined for 28 WN stars. In all cases these ratios are lower

Table 11. See the caption of Table 6

He II i	k	WR16	WR22	WR78	WR40
		EW			
3	4	31(3)	26(12)	36.9(11)	56(12)
3	5	-	-	9.2(9)	7.0(9)
3	6	-	1.9(9)	3.7(9)	4.5(9)
3	7	-	0.75(9)	2.2(9)	3.5(9)
4	5	25(5)	36(7)	57(18)	33(18)
4	6	54(3)	57(12)	44.4(8)	103.5(16,18)
4	7	4.0(4)	3.3(12)	7.7(8)	8.0(4)
4	8	16.6(3)	11(12)	11.8(8,11)	25.7(12,16)
4	9	3.7(3)	1.5(3)	3.6(11)	6.5(16)
4	10	8.0(3)	2.8(3)	5.0(11)	14.2(16)
4	11	-	-	-	3.6(16)
4	14	-	-	1.5(11)	5.1:(16)
4	15	-	-	1.0(11)	1.5:(16)
4	17	-	-	0.7:(11)	-
4	18	-	-	0.8:(11)	-
5	9	-	-	5.7(18)	5.1(18)
5	15	-	-	1.4(11)	1.2(18)
5	16	-	-	1.0:(11)	-
5	17	-	-	0.90(11,18)	1.0(18)
6	10	75(19)	40(19)	41(19)	95(19)
6	12	41(19)	20(19)	6(19)	56(19)
6	14	18.2(18)	6.0(18)	-	-
6	15	1.2(18)	0.43(18)	1.5(18)	1.4(18)
6	22	3.8(18)	0.74(18)	1.2(18)	5.0(18)
6	23	0.30(18)	0.10(18)	0.34(18)	-
6	24	2.9(18)	-	0.72(18)	4.0(18)
6	25	0.53(18)	-	0.33(18)	0.50(18)
6	26	1.5(18)	-	0.34(18)	2.9(18)
7	10	10(19)	17(19)	27(19)	-
7	12	3.0(19)	-	10.1(19)	-
7	14	-	-	9.5(19)	-
8	14	77(19)	43(19)	41(19)	94(19)
8	20	28(19)	-	14.5(19)	32(19)
8	22	19(19)	-	10.8(19)	22(19)
8	24	15(19)	-	9.7(19)	15(19)
8	26	11(19)	-	4.2(19)	15(19)
8	28	9.0(19)	-	5.5(19)	13(19)
8	32	6.0(19)	-	3.5(19)	-
He I					
5876		21(4)	1.3(12)	8.0(4,11)	46(4)
10830		246(5)	30(12)	110(4)	430(12)

Table 12. See the caption of Table 6

He II i	k	WR85	WR155	WR156	WR158
		EW			
3	4	89(2)	34(2)	26.4(2,11)	31(2)
4	5	106.5(7,14)	95.3(5,6)	11.5(5)	26(5)
4	6	78.2(14)	-	84.0(8)	68.5(8)
4	7	15.5(2)	4.5(5)	2.0(2,8)	4.3(8)
4	8	13(3)	-	20.2(8,11)	13.7(8)
4	9	7.8(3)	1.1(3)	4.1(8.11)	3.0(8)
4	10	10(3)	0.44:(3)	9.7(8,11)	5.5(8)
4	14	-	-	3.6(11)	-
4	15	-	-	0.7(11)	-
4	17	-	-	0.7(11)	-
4	18	-	-	1.7(11)	-
5	9	14.0(7,14)	7.1(7)	3.9(7)	5.3(7)
5	11	4.8(14)	-	-	-
5	12	0.8:(14)	2.0(7)	-	-
5	15	2.0(14)	-	-	-
6	12	-	11.7(6)	-	-
6	13	-	4.0(6)	-	1.6(5)
6	14	19.0(14,18)	7.7(6)	16.2(5,7)	7.9(5)
6	15	3.8(14,18)	2.1(6)	1.4(5)	1.3(5)
6	21	0.80(14)	-	-	-
6	22	3.0(14,18)	1.1(5)	3.6(5)	2.0(5)
6	23	0.83(18)	0.56(5)	0.32(5)	0.25(5)
6	24	2.0(18)	0.63(5)	3.2(5)	1.8(5)
6	25	0.58(18)	0.36(5)	0.56(5)	0.32(5)
6	26	0.62(18)	0.56(5)	2.0(5)	1.8(5)
He I					
5876		6.7(14)	1.9(2)	15.5(2,8)	5.8(8)
10830		-	51.9(6)	152(5)	55(5)

as compared to the mean cosmic-value. In the case of WC stars the blending problems are much more complicated as compared to the WN stars, but nevertheless from their decrement graphs we may conclude that hydrogen is not present in their winds. The excesses in some expected He II + H I blends are not seen in other lines of the same series and must therefore be interpreted as blending due to the lines of other elements than H I. In future studies it is needed to improve the wind models by taking into account more realistically the influence of density inhomogeneities. For some stars (indicated by colons in Table 5) it is needed to have better observations of He II and He II + H I line fluxes for getting reliable estimates of H/He ratios. The obtained results confirm the established opinion that WR stars are chemically evolved objects.

Acknowledgements. The authors acknowledge valuable comments and suggestions of the referee W.-R. Hamann. This work was supported by the Polish Committee for Science Research (KBN) under the grant No. 2 2112 92 03 through Nicolaus Copernicus University in Toruń and by the Estonian Science Foundation grant No. 175.

Appendix A: atomic data

A.1. H I

For H I we used an atomic model consisting of 20 distinctly treated bound levels of the principal quantum number n plus H II state. The influence of higher states is taken into account through the correction terms. All H I computations were performed together with He II by the scheme described in Sect. 3 (a 40 level He II atomic model was used in these computations).

Oscillator strengths, collisional excitation rates and photoionization cross-sections were adopted for H I mainly from Johnson (1972), only for collisional excitation and depopulation rates for transitions (1-2) and (1-3) the more correct data

Table 13. Equivalent widths in Å and fluxes in erg cm^{-2} s^{-1}. Code numbers of data sources are given in the brackets (see the end of the table). Uncertain data are indicated by colons

He II		WR 135		WR 111	
i	k	EW	Flux	EW	Flux
3	4	125(1,20)	.853E-09	-	-
3	6	13(9)	.436E-09	16.6(9)	.697E-09
3	7	9.2(9)	.403E-09	16.0(9)	.914E-09
4	5	84.1(5,6)	.571E-10	178(5,6)	.909E-10
4	7	23.0(1,4)	.103E-09	32.3(20,23)	.998E-10
4	8	17.3(1,21)	.106E-09	24.3(20,23)	.105E-09
4	9	13.8(1,21)	.103E-09	17.8(20)	.959E-10
5	16	3.2(20)	.902E-11	7.6(20)	.146E-10
6	9		.139E-10(22)	93(24)	.229E-10
6	10		.122E-10(22)		.268E-10(22)
6	12	20.3(6)	.121E-10		.208E-10(22)
6	13	10.2(6)	.694E-11		
6	14	13.8(6)	.104E-10		
7	10		.522E-11(22)		.519E-11(22)
7	12		.470E-11(22)		.826E-11(22)
7	13		.411E-11(22)		.776E-11(22)
7	14		.347E-11(22)		-
7	16		.255E-11(22)		-
8	13		.180E-11(22)		.200E-11(22)
8	14		.169E-11(22)		.170E-11(22)
9	14		.874E-12(22)		-
He I					
5876		62(1,20)	.215E-09	-	-
10830		280(5,6)	.171E-09	92.3(6)	.389E-10

The data sources:
(1) - Niedzielski & Nugis (1991); (2) - Conti et al. (1989); (3) - Conti et al. (1983); (4) -Schmutz et al. (1989); (5) - Vreux et al. (1990); (6) - Howarth & Schmutz (1992); (7) - Conti et al. (1990); (8) - Hamann et al. (1993); (9) - Niedzielski & Rochowicz (1994); (10) - Smith & Kuhi (1970); (11) - Smith & Kuhi (1981); (12) - Hamann et al. (1991); (13) - Willis & Stickland (1990); (14) - Vreux et al. (1983); (15) - Hillier et al. (1983); (16) - Smith & Willis (1982); (17) - Smith (1955); (18) - Vreux et al. (1989); (19) - Hillier (1985); (20) - Torres (1985); (21) -Nussbaumer et al. (1982); (22) - Eenens & Williams (1992); (23) - Koesterke et al. (1992); (24) - Smith & Hummer (1988).

according to Aggarwal (1983) were used. It must be said that the statement made by Bhatia & Underhill (1986) that the proposed by Johnson (1972) approximate formulae for collisional excitation rates of H I sometimes give negative values was not found to be the case, only exponential integrals in the approximation formulae must be calculated very precisely. As compared to the formulae of van Regemorter (1962), the results of Johnson (1972) are not substantially different.

*A.2. He*II *and He*I

The model atom of He II used in the present study consists of 40 distinctly treated bound levels of the principal quantum number n plus He III state. The influence of higher bound levels was taken into account through the correction terms by the scheme described below. For late type WN stars it is necessary to use at least this number of bound states, otherwise the correction terms cannot be calculated accurately enough and the obtained results are not reliable. This is due to the circumstance that in the case of late type WN stars a substantial contribution into line fluxes comes from the region of the envelope where He III is not the dominating stage.

For He I we used 52 bound levels plus the He II state n=1. Up to $n \leq 4$ all angular momentum states were treated as distinct levels. In the case of $n = 5-8$ all the individual angular momentum states with $l \leq 2$ were treated as distinct levels while the states with $l \geq 3$ were clumped together. The last "buffer level" n = 9 consists of all clumped together singlet and triplet angular momentum states. The influence of higher levels ($n > 10$) was calculated through the correction terms.

For He II we used the hydrogenic formulae (z=2) for radiative transitions, whereas f_{ik} (He II) $\approx f_{ik}$ (H I). For finding collisional excitation and ionization rates (the rates of inverse processes can easily be found from these rates by using conventional formulae) we used the approximation formulae of Klein & Castor (1978), only for collisional ionizations from levels $n \geq 12$ (for which the data were not presented) we used the Seaton formula (1962). For He I the oscillator strengths were adopted from the paper of Green et al. (1966) (the dipole velocity approximation results for transitions $f(nl, n'l')$ with $l, l' \leq 2$ were used) and for transitions between levels $(nl, n'l')$ with $l, l' \geq 2$ the hydrogen oscillator strengths were used. The oscillator strengths for the most important optically forbidden transitions in the LS-scheme were adopted from the sources described in Ilmas & Nugis (1982).

We used for He I the numerical approximation formulae for photoionization cross-sections κ_ν which were derived from the Tables of Peach (1967). For $l > 2$ states the hydrogenic formula and for the ground state 1S the formula proposed by Allen (1973) were used. For collisional excitation rates of He I we used the formulae from Berrington & Kingston (1987) where the data are given for almost all transitions $nl, n'l'$ with $n, n' \leq 3$. For $3^1S - 3^1D$ and $3^1S - 3^3D$ transitions we used the formulae proposed by Vainshtein et al. (1979) and for optically forbidden transitions from 2^3S states into $4L$ states we used the b_{ik} formulae from Auer & Mihalas (1973). For all remaining optically allowed transitions in our atomic model of He I the collisional excitation rates b_{ik} were found by using the formulae of Mihalas & Stone (1968). Collisional ionization rates were also found by using the formulae of Mihalas & Stone (1968).

The rates of dielectronic recombinations and the inverse processes were calculated for He I by the scheme of Ilmas & Nugis (1982).

Appendix B: correction terms

Appendix

In the spectra of WR stars we can observe the lines which arise in transitions between highly excited states. To predict correctly their line fluxes, many levels in atomic models should be used. The influence of higher levels can be taken into account through correction terms.

We calculated the radiative correction terms for some level k according to the following scheme:

$$Cor^r_+(k) = \sum_{j=k_o+1}^{\infty}\left[N_j\left(A_{jk}\beta_{jk}+B_{jk}\beta^c_{jk}\rho^*_c\frac{f_\nu}{f^*_\nu}\right)\right] = \quad (B1)$$

$$= \overline{b'}N_eN_t\overline{\beta}\left(\sum_{j=k_o+1}^{\infty} z^0_jA_{jk}+\right.$$

$$\left.+\frac{\overline{\beta^c}}{\overline{\beta}}\frac{\overline{f_\nu}}{f^*_\nu}\sum_{j=k_o+1}^{\infty}\frac{1}{\exp(h\nu_{kj}/kT_*)-1}\right) ,$$

$$Cor^r_-(k) = N_k\sum_{j=k_o+1}^{\infty}B_{kj}\rho^*_c\beta^c_{kj}\frac{f_\nu}{f^*_\nu} = \quad (B2)$$

$$= N_k\overline{\beta}_c\frac{\overline{f_\nu}}{f^*_\nu}\frac{1}{g_k}\sum_{j=k_o+1}^{\infty}\frac{g_jA_{jk}}{\exp(h\nu_{kj}/kT_*)-1} ,$$

where for finding $\overline{b'}$, $\overline{\beta}$ and $\overline{\beta^c}$ we used the approximations:

$$\overline{b'} = (1-x)(\sqrt{b'_{k_o}}+1)/2 \quad (b=b'(1-x)) , \quad (B3)$$

$$\overline{\beta} = 3.0\beta^{2/3}_{ik_o} \quad \text{if} \quad \beta_{ik_o}\le 0.15 ,$$

$$\overline{\beta} = (\beta_{ik_o}+1)/2 \quad \text{if} \quad \beta_{ik_o} > 0.15 ,$$

$$\overline{\beta^c} = \frac{\beta^c_{ik_o}}{\beta_{ik_o}}\overline{\beta} .$$

In that part of the envelope where the atoms are dominantly ionized we have that $\overline{b'} \approx 1$ if a sufficiently large number of levels is treated in the main system of level population statistical equilibria equations.

Correction terms for the collisional excitation and de-excitation were calculated by the scheme:

$$Cor^c_+(k) = \sum_{j=k_o+1}^{\infty} N_e a_{jk} N_j = \quad (B4)$$

$$= g_kN_e\overline{b'}N_eN_t\sum_{j=k_o+1}^{\infty}\frac{z^0_jb_{kj}}{g_j}e^{\frac{\chi_{kj}}{kT_e}} ,$$

$$Cor^c_-(k) = N_kN_e\sum_{j=k_o+1}^{\infty}b_{kj} . \quad (B5)$$

For He I all the correction terms are proportional to the oscillator strengths and to find them for higher levels for which no data were available, we used the extrapolation scheme. Using the data of Green et al. (1966) for He I oscillator strengths we can conclude by comparing them with the hydrogen oscillator strengths that the ratio $f^{\rm He}(nl,n'l')/f^{\rm H}(nl,n'l')$ tends to become constant when n is high enough for a fixed n'. This is also valid for the ratio $f^{\rm He}[(n^*+n')l,n'l')]/f^{\rm H}[(n^*+n')l,n'l')]$ at high enough n' when n^* is constant ($n^*\ge 1$). These tendencies enable us to get reasonable extrapolations for $f^{\rm He}$ even when n' is close to 8 or 9 for transitions involving the S term which are the highest values of n' for which f_{ik} are given in Green et al. (1966).

References

Abbott D.C., Bieging J.H., Churchwell E., Torres A.V.: 1986, ApJ 303, 239
Aggarwal K.M.: 1983, MNRAS 202, 15P
Allen C.W.: 1973, Astrophysical Quantities, Athlone Press, University of London
Antokhin I.I., Nugis T., Cherepashchuk A.M.: 1992, Astron. Zh. 69, 516
Auer L.H., Mihalas D.M.: 1973, ApJS 25, 433
Barlow M.J., Hummer D.G.: 1982, in "Wolf-Rayet Stars: Observations, Physics and Evolution", Proc. IAU Symp. 99, eds. C.W.H de Loore, A.J. Willis, Dordecht, Reidel, p. 387
Baschek B., Scholtz M., Wehrse R.: 1991, A&A 246, 374
Beals C.S., Plaskett H.H.: 1935, Trans. IAU 5, 184
Berrington K.A., Kingston A.E.: 1987, J. Phys. B. 20, 6631
Bhatia A.K., Underhill A.B.: 1986, ApJS 60, 323
Bhatia A.K., Underhill A.B.: 1988, ApJS 67, 187
Beichmann C.A., Neugebauer G., Habing H.J., Cledd P.E., Chester T.Y.: 1985, IRAS Explanatory Supplement, JPLD - 1855
Boland W., de Jong T.: 1984, A&A 134, 87
Breysacher J.: 1986, A&A 160, 85
Castor J.I.: 1970, MNRAS 149, 111
Castor J.I., Van Blerkom D.: 1970, ApJ 161, 485
Cherepashchuk A.M., Eaton J.A., Khaliullin Kh. F.: 1984, ApJ 281, 774
Cherepashchuk A.M.: 1990, Astr. Zh. 67, 955
Cohen M., Barlow M.J., Kuhi L.V.: 1975, A&A 40, 291
Conti P.S., Leep E.M., Perry D.N.: 1983, ApJ 268, 228
Conti P.S., Massey P.: 1989, ApJ 337, 251
Conti P.S., Morris P.W.: 1990, AJ 99, 898
Conti P.S., Massey P., Vreux J.-M.: 1990, ApJ 354, 359
Crowther P.A.: 1993, PhD Thesis, University of London
Eenens P.R.J., Williams P.M.: 1992, MNRAS 255, 227
Ford G., Stickland D.J.: 1988, in "New Insights in Astrophysics", ESA SP 263, p.502
Garmany C.D., Massey P., Conti P.S.: 1984, ApJ 278, 233
van Genderen A.M., van der Hucht K.A., Steemens W.J.G.: 1987, A&A 185, 131
Green L.C., Johnson N.C., Kolchin E.K.: 1966, ApJ 144, 369
Hamann W.-R., Schmutz W.: 1987, A&A 174, 173
Hamann W.-R., Dünnebeil G., Koesterke L., Schmutz W., Wessolowski U.: 1991, A&A 249, 443
Hamann W.-R., Leuenhagen U., Koesterke L., Wessolowski U.: 1992, A&A 255, 200
Hamann W.-R, Koesterke L., Wessolowski U.: 1993, A&A 274, 397
Hamann W.-R, Koesterke L., Wessolowski U.: 1994, A&A (in press)
Hayes D.C., Latham D.W.: 1975, ApJ 197, 593
Hershkowitz S., Linder E., Wagoner R.V.: 1986, ApJ 303, 800
Hillier D.J., Jones T.J., Hyland A.R.: 1983, ApJ 271, 221
Hillier D.J.: 1985, AJ 90, 1514
Hillier D.J.: 1988, ApJ 327, 821
Hillier D.J.: 1989, ApJ 347, 392
Hillier D.J.: 1991, A&A 247, 455
Hogg D.E.: 1989, AJ 98, 282
Holm A.V., Cassinelli J.P.: 1977, ApJ 211, 432

Howarth I.D., Schmutz W.: 1992, A&A 261, 503
Hua C.T., Woo J.O., Nguyen H.D.: 1983, A&AS 53, 407
van der Hucht K.A., Conti P.S.,Lundström I., Stenholm B.: 1981, Space Sci. Rev. 28, 227
van der Hucht K.A., Hidayat B., Admiranto A.G., Supelli K.R., Doom C.: 1988, A&A 199, 217
van der Hucht K.A.: 1992, Ann. Rev. Astron. Astrophys. 4, 123
Ilmas M., Nugis T.: 1982, Tartu Astrofüüs. Obs. Teated 67, 3
Johnson L.C.: 1972, ApJ 174, 227
Klein R.L., Castor J.I.: 1978, ApJ 220, 902
Koesterke L., Hamann W.-R. Wessolowski U.: 1992, A&A 261, 535
Kuhi L.V.: 1966, ApJ 143, 753
Leitherer C., Robert C.: 1991, ApJ 377, 629
Lundström I., Stenholm B.: 1984, A&A 58, 163
Maeder A.: 1985, A&A 147, 300
Massey P.: 1980, ApJ 236, 526
Massey P.: 1984, ApJ 281, 789
Mihalas D.M., Stone M.E.: 1968, ApJ 151, 293
Moffat A.F.J., Drissen L., Robert C.: 1988, ApJ 334, 1038
Moffat A.F.J., Robert C.: 1991, in "Wolf-Rayet Stars and Interrelations with Other Massive Stars in Galaxies", Proc. IAU Symp. 143, eds. K.A. van der Hucht, B. Hidayat, Kluwer, p. 109
Niedzielski A., Nugis T.: 1991, A&AS 91, 273
Niedzielski A., Rochowicz K.: 1994 A&AS 108, 669
Nugis T.: 1984, Publ. Tartu Astrofüüs. Obs. 50, 101
Nugis T.: 1988, Tartu Astrofüüs. Obs. Teated 89, 89 (in russian)
Nugis T.: 1990a, Astrofizika 32, 85
Nugis T.: 1990b, Publ. Tartu Astrofüüs. Obs. 53, 79
Nugis T.: 1991, in "Evolution of Stars: the Photospheric Abundance Connection", Proc. IAU Symp. 145, eds. G. Michaud, A. Tutukov, Kluwer, p. 209
Nussbaumer H., Schmutz W., Smith L.J., Willis A.J.: 1982, A&AS 47, 257
Peach G.: 1967, MNRAS 71, 13
Pitault A., Epchtein N., Gómez A., Lortet M.C.: 1983, A&A 120, 53
Prinja R.K., Barlow M.J., Howarth I.D.: 1990, ApJ 361, 607
van Regemorter H.: 1966, ApJ 136, 906
Robert C., Moffat A.F.J.: 1990, in "Intrinsic Properties of Hot Luminous Stars", ASP Conf. Ser. 7, ed. C. Garmany, p. 271
Sapar A., Kuusik I.: 1978, Publ. Tartu Astrofüüs. Obs., 40, 71
Schmutz W., Hamann W.-R., Wessolowski U.: 1989, A&A 210, 236
Schmutz W.: 1991, in "Stellar Atmospheres: Beyond Classical Models", NATO Advanced Research Workshop, eds. L. Crivellari, I. Hubeny, D.G. Hummer, Kluwer, p.191
Schmutz W., Vacca W.D.: 1991, A&AS 89, 259
Seaton M.J.: 1962, The Theory of Excitation and Ionization by Electron Impact, in "Atomic and Molecular Processes", ed. D.R. Bates, New York, Academic Press
Seaton M.J.: 1979, MNRAS 187, 73P
Smith H.J.: 1955, Thesis, Harvard University, Cambridge
Smith L.F.: 1968a, MNRAS 138, 109
Smith L.F.: 1968b, MNRAS 141, 317
Smith L.F., Kuhi L.V.: 1970, ApJ 162, 535
Smith L.F., Kuhi L.V.: 1981, An Atlas of Wolf-Rayet Line Profiles, JILA Report 117, University of Colorado
Smith L.F., Hummer D.G.: 1988, MNRAS 230, 511
Smith L.J., Willis A.J.: 1982, MNRAS 201, 451
Torres A.V.: 1985, Thesis, JILA, Colorado
Torres-Dodgen A.V., Massey P.: 1988, AJ 96, 1076
Underhill A.B.: 1983, ApJ 266, 718
Underhill A.B.: 1991, in "Wolf-Rayet Stars and Interrelations with Other Massive Stars in Galaxies", Proc. IAU Symp. 143, eds. K.A. van der Hucht, B. Hidayat, Kluwer, p. 53
Vacca W.D., Torres-Dodgen A.V.: 1990, ApJS 73, 685
Vainshtein L.A., Sobelman I.I., Yukov E.A.: 1979, in "Atomic Excitation and Spectral Line Widening" Nauka, Moscow (in russian)
Vreux J.-M., Dennefeld M., Andrillat Y.: 1983, A&AS 54, 437
Vreux J.-M., Dennefeld M., Andrillat Y., Rochowicz K.: 1989, A&AS 81, 353
Vreux J.-M., Andrillat Y., Biemont E.: 1990, A&A 238, 207
Williams P.M., Antonopoulou E.: 1981, MNRAS 196, 915
Williams P.M., van der Hucht K.A., Thé P.S.: 1987, A&A 182, 91
Willis A.J., van der Hucht K.A., Conti P.S., Garmany C.D.: 1986, A&AS 63, 417
Willis A.J., Stickland D.J.: 1990, A&A 232, 89

This article was processed by the author using Springer-Verlag LaTeX A&A style file version 3.